National Library
of Canada

Acquisitions and
Bibliographic Services Branch

395 Wellington Street
Ottawa, Ontario
K1A 0N4

Bibliothèque nationale
du Canada

Direction des acquisitions et
des services bibliographiques

395, rue Wellington
Ottawa (Ontario)
K1A 0N4

*Your file* *Votre référence*

*Our file* *Notre référence*

## NOTICE

The quality of this microform is heavily dependent upon the quality of the original thesis submitted for microfilming. Every effort has been made to ensure the highest quality of reproduction possible.

If pages are missing, contact the university which granted the degree.

Some pages may have indistinct print especially if the original pages were typed with a poor typewriter ribbon or if the university sent us an inferior photocopy.



## AVIS

La qualité de cette microforme dépend grandement de la qualité de la thèse soumise au microfilmage. Nous avons tout fait pour assurer une qualité supérieure de reproduction.

S'il manque des pages, veuillez communiquer avec l'université qui a conféré le grade.

La qualité d'impression de certaines pages peut laisser à désirer, surtout si les pages originales ont été dactylographiées à l'aide d'un ruban usé ou si l'université nous a fait parvenir une photocopie de qualité inférieure.



Canada

# THE GEOCHEMISTRY OF SHOCKED AND COUNTRY ROCKS FROM THE LAKE WANAPITEI IMPACT STRUCTURE, ONTARIO

- by -

Tomasz Jan Ber

A thesis submitted to the School of Graduate Studies and Research in partial fulfillment of the requirements for the degree of Master of Science

UNIVERSITY OF OTTAWA

ISBN 0-315-85784-6

Canada

UNIVERSITÉ D'OTTAWA
UNIVERSITY OF OTTAWA

## ABSTRACT

Lake Wanapitei is located in central Ontario, 40 km northeast of Sudbury. It has been recognized as an impact structure formed approximately 37 Ma ago from a hypervelocity impact of possibly an LL-chondrite. The geophysical and morphological evidence suggest that the crater originally measured 8500 m in diameter. The original ground surface has been lowered by some 300 m; material scoured from the crater floor has been deposited as glacial float on and south of the southern shoreline. The shock metamorphosed rock fragments in these deposits consist of glassy melt rocks and suevitic breccias with lithic clasts of mainly quartzite, arkose, wacke, siltstone, and diabase. This work concentrates on establishing a compositional relationship between the Wanapitei crater lithologies and the unshocked country rocks at the area. Due to the relatively young age of the structure, the impact melt glasses are well preserved, with a low content of quench plagioclase and other alterations resulting from devitrification. Presented here are the results of bulk rock XRF and microprobe analyses of the Wanapitei crater rocks together with analyses of country rocks, that may have been exposed to the impact at the time of event. The suspected target rocks are represented by Proterozoic quartzitic sediments of Mississagi, Bruce, and Gowganda Formations, and diabase dikes of Nipissing

Intrusions. A least-squares mixing model has been applied to determine which of the country rocks, were mixed to produce the observed impact glass lithologies. The results indicate 56% of Mississagi and 44% of Gowganda Formations; however, secondary evidence suggests a limited contribution of the Nipissing rocks. Based on these results, the meteoritic content of the impact melts has been established, and by comparison of siderophile geochemical data with the Wanapitei samples, a chondrite has been confirmed as the most probable projectile. The grade of shock metamorphism recorded in the Wanapitei shocked rocks suggests at least 65-70 GPa for maximum pressures and up to 2500°C for maximum temperatures.

# SOMMAIRE

Le lac Wanapitei est situé dans le centre de l'Ontario à 40 km au nord-est de Sudburry. Il a été identifié comme une structure d'impact formé par un impact à hyper-vélocité, de possiblement une chondrite-LL, il y a environ 37 millions d'années. Les évidences géophysiques et morphologiques suggèrent que le cratère mesurait 8500 m de diamètre à l'origine. La surface originale du sol a été abaissé d'environ 300 m et du matériel arraché du fond du cratère déposé comme débris glaciaires sur la rive sud. Les fragments de rocs sujets au métamorphisme de choc de ces dépôts se composent de fondres vitrifiés et de brèches suévitiques avec des clastes lithiques de surtout de gres, quartzite, arkose, wacke, siltstone et de diabase. Ce travail porte sur la détermination d'une relation entre la composition des lithologies du cratère Wanapitei et les roches de la région. Étant donné l'âge relativement jeune de la structure, les verres de fondres d'impact sont bien préservés, avec un faible contenu en "plagioclase quench" et autres altérations dues à la vitrification. Les résultats d'analyses par la methode XRF et par microprobe des roches du cratère Wanapitei ainsi que les analyses des roches de la région qui peuvent avoir été soumis à l'impact sont présentés. Les roches que l'on pense d'impacts sont représentées par des sédiments quartzitiques de Mississagi, les formations de Bruce et Gowganda, et les dykes intrusifs de diabases de Nipissing. Un modèle de mélange par moindres carrés à été utilisé pour déterminer lesquelles des roches de la région, et dans quelle proportion, ont étées mélangées pour produire les lithologies d'impact observées. Les résultats indiquent 56.4% de la formation de Mississagi et 43.6% de la formation de Gowganda; cependant, une évidence secondaire suggèrent une participation limitée des roches du Nipissing. En se basant sur ces résultats, le contenu météoritique des fondres d'impact a été déterminé et en comparant les données sidérophiles géochimiques avec les échantillons de Wanapitei, on confirme qu'une chondrite est le projectile le plus probable. Le niveau de métamorphisme de choc observé dans les roches d'impact de Wanapitei suggère des pressions de 65 à 70 GPa et une température jusqu'à 2500$^{o}$ C.

## Acknowledgements

I would like to thank Richard A.F. Grieve for his constructive help, criticism, advice, and encouragement on the way to complete this study. I would also like to acknowledge Ralph Kretz, Blyth Robertson, and Mark Mihalasky for a great deal of help and advice, for which I am very grateful. I address special thanks to Staff of the Geological Survey of Canada for help and support in undertaking the work.

# TABLE OF CONTENTS

# LIST OF TABLES

# LIST OF ILLUSTRATIONS

## I. FIGURES

II. PLATES

# General Introduction

Small terrestrial impact craters with associated meteorite fragments have been recognized since the 1930's. Larger craters first were identified in the 1940's (1947, discovery of shatter cones at Kentland structure by R.S. Dietz; Melosh, 1989) and later in 1960's when the association of hypervelocity impact and shock metamorphism was established (experimental production of shatter cones by E.M. Shoemaker and others in 1961). The most intensive research of terrestrial impact structures took place, however, after data became available from the Moon, and other bodies of the Solar system, which drew attention to the importance of impact as a planetary geologic process.

The study of impact structures has identified many characteristics, such as shock metamorphism, which occur as part of the impact process. Data from the Moon dismissed the suggestion of a volcanic origin for a large number of lunar craters, favouring instead the concept of meteoritic impact origin. Like the Moon, the Earth must have experienced a meteoritic bombardment similar in size and intensity. However, unlike the Moon, the Earth has a very active geological environment in which the atmosphere, water and ice, plate tectonics, intensive chemical and physical weathering continuously destroy evidence of the meteoritic bombardment of

the planet. In addition, smaller projectiles burn up in the Earth's atmosphere, never reaching the planetary surface, or if they do, it is with reduced cosmic velocity. The projectiles that impact the oceans result in craters hidden from direct observation; smaller impacts do not form craters at all.

Since the early 1970's, Lake Wanapitei area has been regarded as an impact structure (Dence and Popelar, 1972). It represents an impact site which, although relatively young, has been extensively modified by erosion. The previous presence of a crater is suggested by a gravity anomaly, characteristic concentric tectonic disturbance of the area, and near-by loose fragments that have been affected by shock metamorphism.

## Previous Research on Lake Wanapitei

Previous research on the Lake Wanapitei area dates back to 1853-56 and 1890, when A.Murray and later R.Bell, carried out the earliest geological reconnaissance of the area (Murray, 1853-56; Bell, 1891). In 1913, W.H. Collins published the results of his studies of the area south of the lake (Collins, 1913). Until 1971, mapping and exploration led to the discovery of Au, Cu, Ag, Pb, U, Ni, and Fe (Koulomzine, 1955; Ogden, 1957). Popelar (1971) reported gravity measurements of the Sudbury area, revealing a distinct Bouguer gravity anomaly centered over Lake Wanapitei. In 1972, Dence and Popelar reported evidence for an impact origin of the structure, based on gravity measurements, and on topographic, and petrographic data.

The presence of coesite (a high pressure polymorph of quartz) in melt glasses from Lake Wanapitei were reported by Dence et al. (1974). Winzer et al. (1976) presented the results of K/Ar isotopic dating of the melt glasses, estimating the time of the impact event at approximately 37 Ma. Wolf et al., (1980) attempted to identify the projectile, based upon trace-element abundances in impact melt glass samples, and suggested LL-chondrite as the most probable projectile that formed the crater. Dressler (1982) has described the geology of the Wanapitei Lake area in considerable detail, including a brief interpretation of the impact origin of the lake basin. "Special

Volume no.1" on "The Geology and Ore Deposits of the Sudbury Structure", by Pye et al., published by the Ontario Geological Survey in 1984 is the latest publication that compiles the present state of knowledge about the Sudbury Structure, with inclusion of the Lake Wanapitei crater in the northeastern corner as the integral part of the geologic history of the region.

## Present Work

The purpose of this work is to further explore details of the Lake Wanapitei impact structure, in particular to establish the compositional relationship between the crater lithologies and the country rocks. The task was centered on a compilation of the available data on the Lake Wanapitei area, which is scattered throughout the earlier publications. Petrographic and chemical analyses were performed on samples of shock metamorphosed rocks from collections of the Ontario Geological Survey, Geological Survey of Canada and samples collected by the author. The method for establishing the target-impact melt rock compositional relationship was based on application of a least squares-mixing model (Wright and Doherty, 1970). The most probable target lithologies were selected from among the possibilities suggested by previous researchers (Dence and Popelar, 1972; Winzer et al, 1976; Wolf et al., 1980). The mixing model provided evidence for the identification of which target rocks melted during the impact event. The geochemical data were further used to identify the projectile by defining the meteoritic content in the impact melted rocks, after corrections for the indigenous content of "meteoritic" elements in the target rocks. In addition, on the basis of petrographic observations and chemical analyses, the pressure and temperature conditions of the Wanapitei impact event, as recorded in the recovered samples, were investigated.

## Methodology

1. Field sampling was carried out during the 1990 field season. Samples of shocked rocks were collected from glacial till along 1500 m of CN railway line south of Lake Wanapitei in the southern part of the village of Skead, Latitude 46°38'45"N and Longitude 80°45'30"W (Figure 1 and Plate I).

2. Thin sections of shocked rocks and country rocks were studied under the transmitted light microscope. Planar features in quartz were measured using a universal stage.

3. Microprobe analyses were obtained on carbon-coated polished thin sections using the McGill University Cameca instrument. The conditions for analysis were: 15 kv accelerating voltage, defocused beam of 5$\mu$M diameter; counting time was set at 50 seconds for all elements except for Si and Al (25 seconds). K$\alpha$ emission lines were measured on all of the analyzed elements.

4. The whole rock analyses were undertaken in the laboratories of the Geological Survey of Canada. The analytical laboratory method was XRF wavelength dispersive analysis of fused disks. The FeO, $H_2O(T)$, $CO_2(T)$, and S were analyzed by rapid chemical methods. $Fe_2O_3$ was calculated using the formula:

$Fe_2O_3 = Fe_2O_3(T(XRF)) - 1.11134 \times FeO(volumetric)$.

Trace elements were determined in the same laboratory by use of the ICP-TRI method. The analyses were made on 1.0 g of sample (acid disolution + fusion of residue) dissolved in 10% HCL and

diluted to 100 ml. Rare-earth elements were determined by the XRF method. Considering the loss of glass under the microprobe electron beam and associated lower values of totals, the whole rock "character" of the XRF analyses, as well as the "geochemical character" of the available target data in literature, the XRF results were chosen to represent the crater lithologies in the mixing model calculations.

Plate I. Glacial float deposits with concentration of shocked rocks, village of Skead area, southern margin of Lake Wanapitei.

The data on Wanapitei target rocks were taken from the literature (Speers, 1957; Thomson, 1961; Young, 1969; Card et al., 1977; Card, 1978; Junnila, 1990).

5. The mixing model calculations were carried out with the computer program of Wright and Doherty (1970), which uses a least squares procedure to combine several country rock types plus meteoritic elements to match the observed composition of impact lithologies.

Figure 1. Geology of the Lake Wanapitei area (based on Dressler, 1982 and Pye et al., 1984).

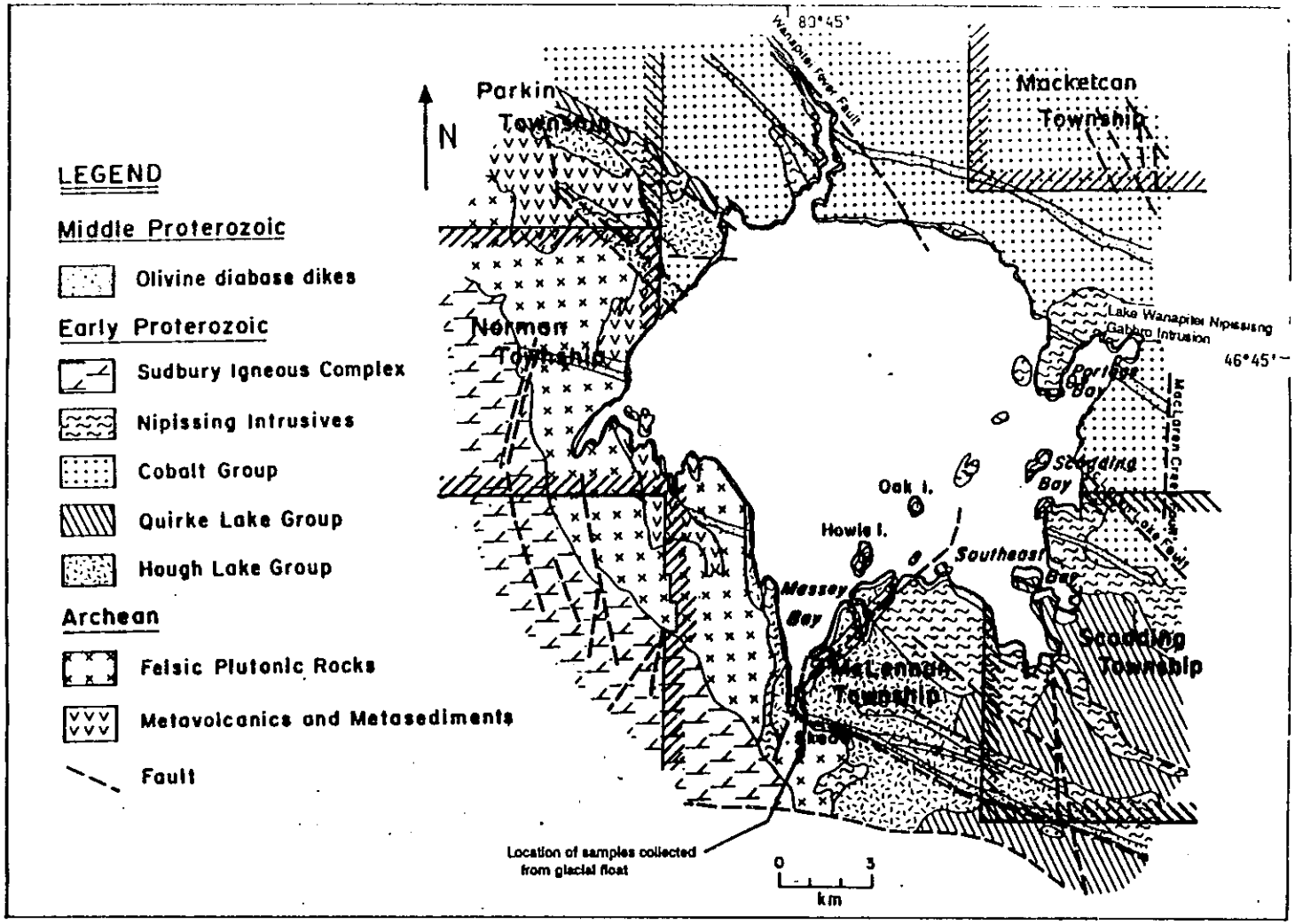

## Location and General Description of the Area.

Lake Wanapitei is located in central Ontario, 40 km northeast of Sudbury, between Latitudes 46°38′ and 46°54′N and Longitudes 80°33′ and 80°51′W. Part of the depression, in which the lake presently resides, evidently represents a segment of a crater that formed as a result of a hypervelocity impact of a meteorite approximately 37 Ma ago (Winzer et al., 1976). The general topography of the area is controlled in part by the structure and lithology of the underlying rocks. Elevations are between 260 and 503 m above sea level. The maximum local relief is 150 m, west of Dewdney Lake in northwestern part of Mackelcan Township (not shown on the included maps). The morphology of the area is well documented on 1:50,000 topography maps issued in 1975, by Survey and Mapping Branch, Department of Energy, Mines and Resources, Canada. The complete Wanapitei Lake area is covered by maps 41-I/15 and 41-I/10.

The lake has a semi-circular northern shoreline and a highly irregular southern margin (Figure 1). Current expression of the impact crater is limited by modifications due to erosion. The deepest part of the lake, located north of the Massey Bay, reaches more than 350 m (Figure 2). Several islands are present in the southeastern part of the lake (Figure 1), approximating a NE-SW oriented linear pattern between Portage Bay and Massey Bay, and possibly expressing the southern outline of the base of

the original crater rim. A few more islands are distributed along the western and northern shorelines. Many small lakes and streams around the Lake Wanapitei delineate a well developed concentric and less pronounced radial pattern of fractures from moderate, possibly impact related, tectonic disturbance of the area, as described by Dence and Popelar (1972). The rivers entering and discharging from the lake are distributed radially. Relatively little drainage to the lake is provided mainly by the Wanapitei River, which enters from the north and discharges to the south. Most of the area surrounding the lake is covered by woods, with little open space remaining. The surficial deposits are Pleistocene glacial sediments, deposited in moraines mostly south of the lake, and Recent swamp, lake, and stream deposits. Bedrock outcrops are present throughout the entire area, in small hills and open exploration pits. Shocked material, which presumably represents Wanapitei crater lithologies, such as impact melt rock and suevite, is found in the Pleistocene glacial drift on the southern margin of the lake, particularly near the village of Skead (Figure 1).

## The Lake Wanapitei Impact Structure

Based on gravity profiles, the original size of the crater was estimated to be 8.5 km in diameter and 3300 m in true depth (Dence and Popelar, 1972, p.122). Thus, the Lake Wanapitei crater evidently was a medium-size impact structure. At present, there is no topographic evidence of central uplift. Since the time of formation, the structure has been extensively modified by erosion. Lake Wanapitei presently measures approximately 10 km in diameter, and its shoreline does not represent the original outline of the post impact structure (Figure 2). The central part of the lake, the area without islands, where water depths exceed 50 m (Figure 2), is considered to be the remaining part of the crater (Dence and Popelar, 1972). Gravity measurements obtained by Popelar (1972), revealed a residual negative Bouguer gravity anomaly of -15 mgal (Figure 3) centered over the Lake Wanapitei (Figure 2). Usually, the negative Bouguer anomaly associated with a crater is the result of relatively low density breccia and fractured rock beneath the crater (Melosh, 1989). In the case of the Wanapitei structure, the density model applied by Dence and Popelar (1972), assumed a two-layered body displaying density contrast with the country rocks of $-0.25 g/cm^3$ for the upper layer, and $-0.15 g/cm^3$ for the lower layer, in a basin 7.50 km in diameter (Figure 3).

The structural configuration of the Wanapitei impact site,

derived from the density model and considerations of other Canadian impact sites, suggests a crater characterized by a central peak with a surrounding annulus of impact breccia. The original ground plane of the crater before erosion was estimated at approximately 300 m higher level than at present, although the model-derived central uplift has not been confirmed by the data on bathymetry (Figure 2). However, based exclusively on this information, it is difficult to reject the possibility of its existence. The transition size from a simple to a complex crater for Earth occurs between 2 and 4 km of diameter (Grieve, 1987, p.248). Thus, the central uplift in the Wanapitei crater could have been developed but was later destroyed by glacial erosion or could be buried by glacial or post-glacial debris. Many features of the Wanapitei impact structure are similar to other Canadian craters of comparable size. Drill cores from Deep Bay and Nicholson Lake impact structures provide lithological and structural analogies for modelling of the Wanapitei crater (Dence and Popelar, 1972). For example, the area of moderate tectonic disturbance around Wanapitei crater reaches up to 18 km in diameter, similar to the 20 km aureole at Deep Bay (Innes et al., 1964). Lac Couture underwent a similar process of degradation by glacial action that removed shocked material from the crater's floor and deposited it away from the structure (Beals et al., 1967).

Figure 2. Bathymetry and Bouguer gravity anomaly, Lake Wanapitei (from Dence and Popelar, 1972 and Robertson and Grieve, 1975).

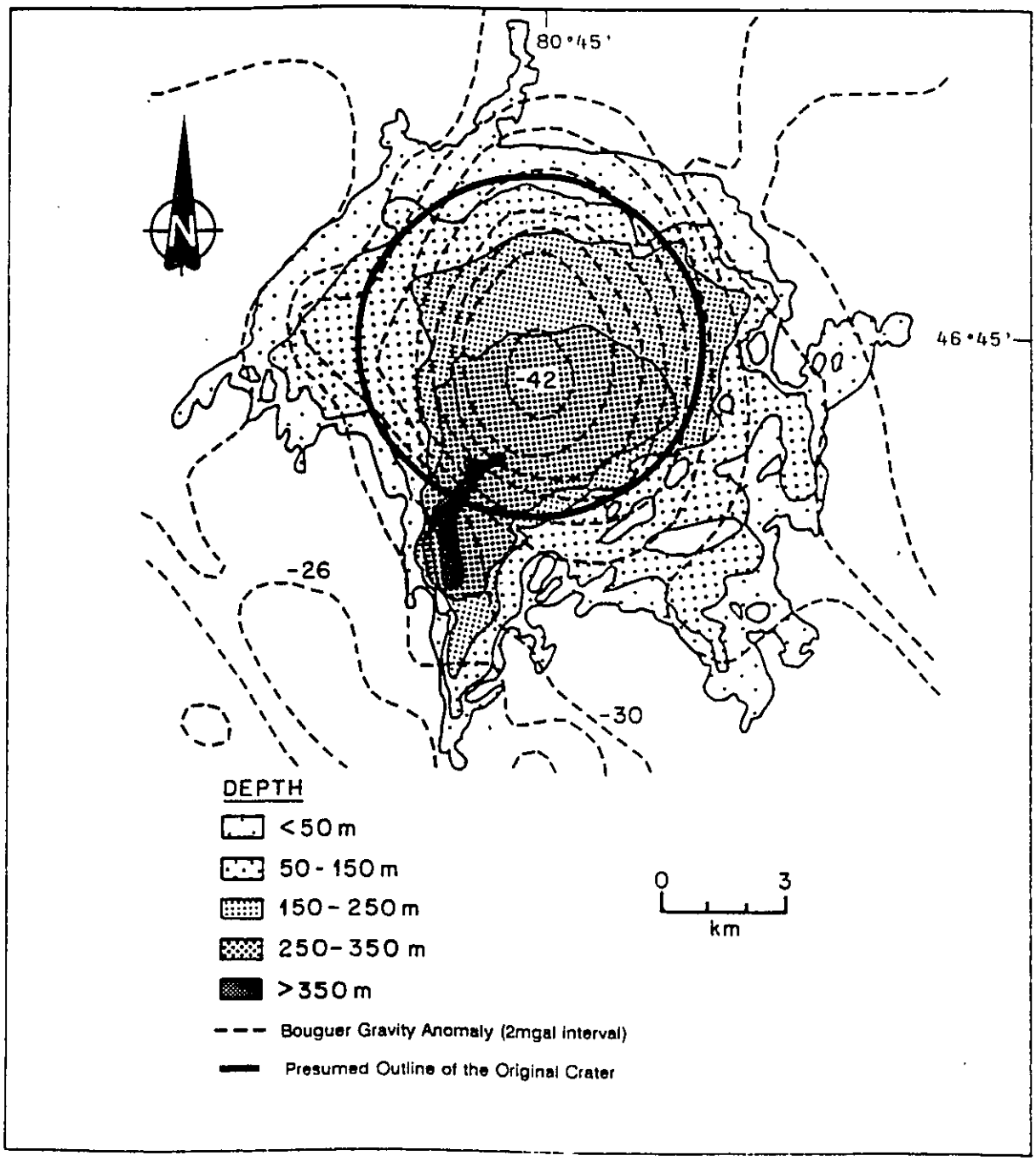

Figure 3. Density and structural models of the Wanapitei crater presented as NE-SW profile across the centre of the Lake Wanapitei (Dence and Popelar, 1972).

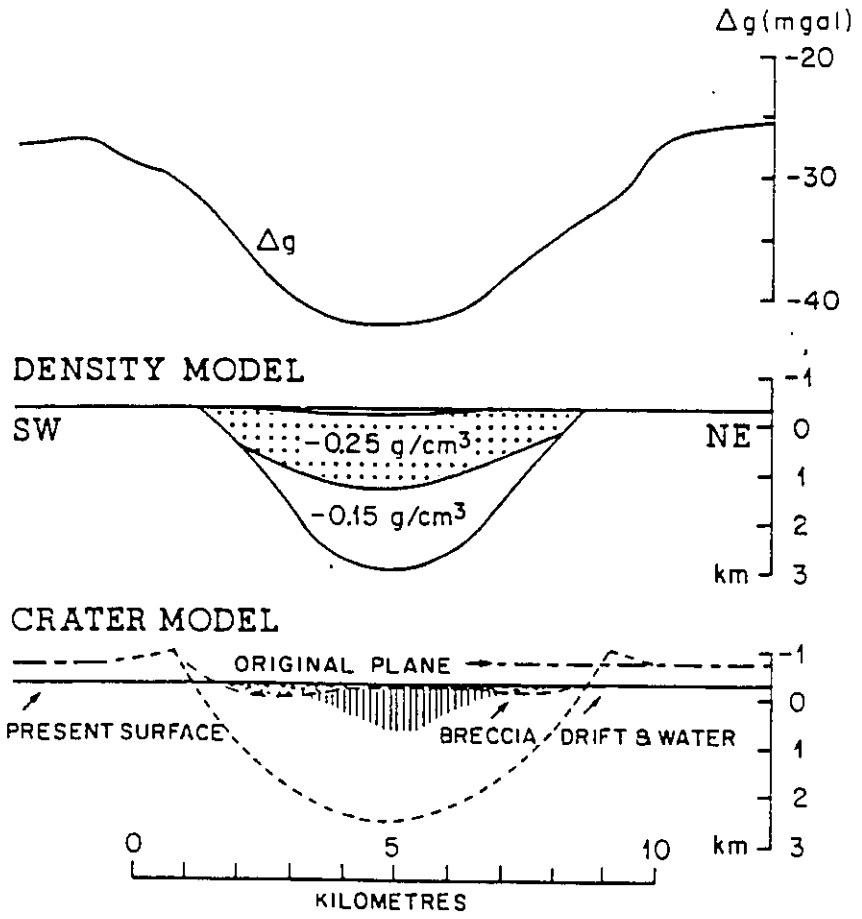


Δg - Bouguer gravity anomaly

The age of the Wanapitei crater was estimated at 37 Ma from K/Ar dating performed on fresh glass veins and glassy whole-rock samples (Winzer et al., 1976). The net meteoritic content of the shocked melted materials, derived from enrichment in meteoritic elements such as Ir, Os, and Ni, suggest an Apollo type body of LL-chondrite composition as the most probable projectile type (Wolf et al., 1980).

## Geology of the Lake Wanapitei Area.

A simplified geology map of the area is shown in Figure 1. The main rock types underlying the Lake Wanapitei area and the immediate surroundings are Archean metavolcanic rocks, metasediments, and felsic plutons to the west, unconformably overlain by Early Proterozoic sedimentary rocks of the Huronian Supergroup in the centre and to the east. The Archean rocks constitute a part of the Superior Structural Province, whereas the Early Proterozoic rocks belong to the Southern Structural Province. The Superior and Southern Provinces meet along a northwesterly trending line (Plate II). Approximately 15 km southwest of the lake, the NE-SW trending Grenville Front Tectonic Zone forms the southern boundary between the Grenville and Southern Structural Provinces (Plate II). The north-northwest striking rocks of the Superior Structural Province, were deformed about 2500 Ma ago, during the late stages of the Kenoran Orogeny (Stockwell et al., 1970). The Sudbury impact event, approximately 1850 Ma ago, caused extensive faulting and brecciation of these units. The Penokean Orogeny, 1800-1600 Ma ago, compressed the Sudbury Structure to its asymmetrical shape (Gibbins and McNutt, 1975). In the Lake Wanapitei area, the Southern Province is represented by Huronian strata that form the eastern end of the orogenic Penokean Fold Belt. The belt underlies the central and eastern parts of the Wanapitei

structure. The Wanapitei crater evidently affected the eastern margin of the Sudbury Igneous Complex (Figure 1 and Plate II) approximately 37 Ma ago.

According to previous concepts, the main targets for the impact were quartzitic sediments of the Huronian Supergroup and dikes of the Nipissing Intrusions (Dence and Popelar, 1972; Winzer, 1975; Wolf et al., 1980). Most of the concentric and radial tectonic discontinuities surrounding Lake Wanapitei are presently occupied by postglacial lakes and streams.

In the northern and eastern part of the Lake Wanapitei depression, the major structural discontinuities are the MacLaren Lake (Figure 1), Laundry Lake (beyond the area of the included map), Wanapitei River, and the MacLaren Creek Faults. Their prevailing trends are north, to north-northwest. The general strike of the southern faults (Figure 1) is west-northwest to northwest, dipping northeasterly. Some of the faults, like the Wanapitei River Fault, continue on both sides of the Lake Wanapitei depression. Dressler (1982) noticed a more complicated structures in the southern part of the Wanapitei area.

Plate II. Regional geological setting of the Lake Wanapitei structure (radar image; Energy, Mines and Resources Canada).

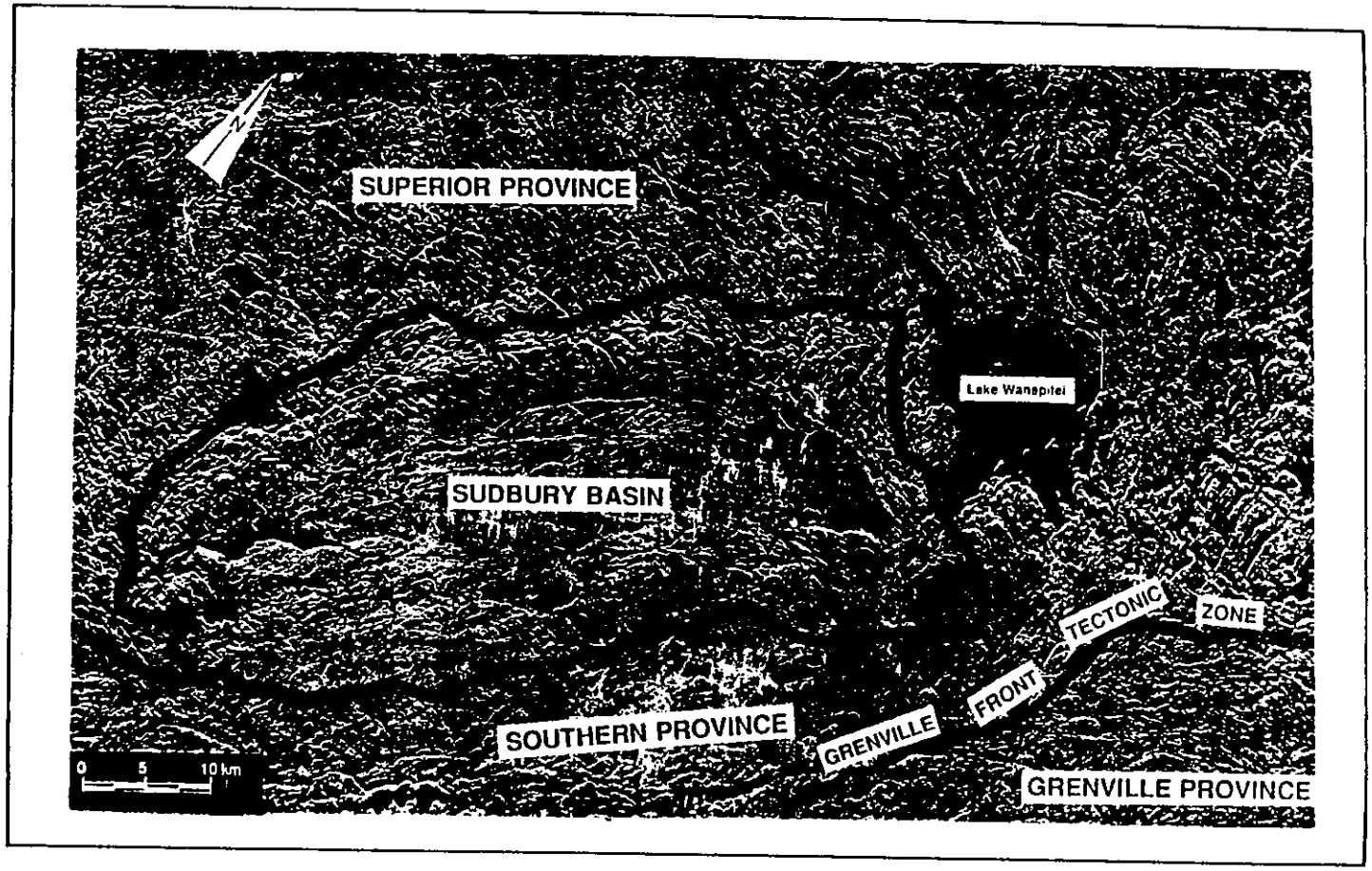

Archean

The oldest in the area are the Archean metavolcanic rocks and metasediments subdivided into mafic, intermediate metavolcanic, and felsic metavolcanic rocks, and metasediments. The mafic and intermediate metavolcanics are present intermittently. Their original structures are obliterated by metamorphism and deformation. The felsic metavolcanics occur in northeastern Norman Township (Dressler, 1982; Meyn, 1970). They have been described as felsic and porphyritic flows rich in plagioclase and lithic fragments (Meyn, 1970). The metasediments are known from west of Lake Wanapitei and south of the village of Skead (Figure 1). They are meta-wacke, meta-arkose, ironstone, ferruginous chert, and paragneiss. The meta-wacke (with metamorphic biotite) shows a gradual transition to a massive to poorly laminated quartz meta-siltstone. The ironstone (consisting of quartz, magnetite, hematite, carbonate, minnesotaite, stilpnomelane) and ferruginous chert (of quartz interbedded with red jasper) occur with metavolcanic rocks in a northwesterly trending zone through Parkin Township (Dressler, 1982).

Gneiss is observed in the western margin of the metavolcanic-metasediment sheet shown in Figure 1. It is brecciated and rarely displays bedding. The second unit of the Archean consists of felsic plutonic rocks, which have an intrusive contact with the metasediments and metavolcanic rocks. The main lithologies

are granite and migmatite. Gradation from granite to migmatite is common. The rocks are exposed along the southwestern part of the lake. Gradation to migmatite is expressed by an enrichment in granite and granodiorite dikes, veins, and patches.

The youngest Archean units are mafic intrusions comprising diabase in three textural varieties (diabase, glomeroporphyritic diabase, and porphyritic diabase). The dikes, which are not shown in Figure 1, are up to several metres thick, and cut felsic plutons south and west of Lake Wanapitei. The emplacement of the dikes occurred along the northwesterly oriented faults and joints. The diabase displays a characteristic sub-ophitic plagioclase-pyroxene microstructure; the glomeroporphyritic and porphyritic varieties display plagioclase organized in clusters or idiomorphic phenocrysts set in a fine matrix.

Proterozoic

In the Lake Wanapitei area, this eon is represented by the early Proterozoic **Huronian Supergroup**, an assemblage of sedimentary and volcanic rocks deposited between 2500 and 2150 Ma ago (Dressler, 1984, p.64). In the Lake Wanapitei area, only the sedimentary lithologies are present. The sedimentation occurred in four cycles recognized as the groups of: Elliot Lake, Hough Lake, Quirke Lake, and Cobalt. In the area of interest, the Elliot Lake Group is absent.

The Mississagi Formation of the **Hough Lake Group** trends southeasterly on the east side of Massey Bay, dipping up to 75°N-NE. It forms most of Howie Island and Oak Island, and continues northwesterly from the northern margin of Lake Wanapitei (Figure 1). The sediments are sandstone, arkose, and wacke with minor conglomerate. Palonen (1971) and Card (1977) described the formation as coarsening upward cyclical sediments of sandstone and minor siltstone. The thickness of the formation estimated from Howie Island (Figure 1) and Red Rock Point (to the south) is a minimum of 1050 m (Dressler, 1982). The sandstone outcrops between Massey Bay and Scadding Township. Numerous interbeds of the coarser wacke and arkose indicate deposition in an active fluvial environment. Lithic fragments in these rocks include quartzite, chert, argillite, siltstone, granite, and felsic metavolcanics.

Mississagi quartzite (of the Mississagi Formation), although not very abundant, is regarded as having been one of the principal target rocks during the impact event. It consists of 95% quartz, set in partially sericitized detrital matrix with feldspars and opaque minerals, mostly pyrite. The relative abundance of a very similar quartzite in the sampled Pleistocene glacial float south of the Lake Wanapitei suggests the possibility that the Wanapitei area was underlaid by Mississagi strata before impact and erosion.

The **Quirke Lake Group** is subdivided into Bruce, Espanola, and Serpent Formations.

Most units of the group dip approximately 30° to 70°N. Out of this group of sediments, the Bruce Formation is the most suitably located to constitute a part of the Wanapitei impact target area. It overlies conformably sediments of the Mississagi Formation, and outcrops in south Scadding Township and southeastern of Parkin Township (Figure 1). The main rock types are conglomerate, pebbly wacke, arkose, and wacke. The conglomerate and pebbly wacke are of glacial origin (Frarey and Roscoe, 1970). They contain clasts of granite, gabbro, quartzite, and metavolcanic rocks set in an arkosic-wacke matrix.

The Espanola Formation comprises calcareous siltstone, limestone, and calcareous wacke. The rocks are in and south of Scadding, Maclennan, and Parkin Townships (Dressler, 1982).

The calcareous siltstone and calcareous wacke are interbedded, displaying fine lamination. The limestone is weakly metamorphosed with a characteristic presence of phlogopite (Dressler, 1982).

The Serpent Formation, which consists of arkose and minor conglomerate, is exposed in Scadding and Parkin Townships. The arkose contains 25-40% of feldspar, rare carbonates, and

sericitic matrix with opaque minerals, interbedded with the arkosic wacke and calcareous arkose. The conglomerate reported by Dressler (1982) from Southeast Bay, contains arkosic, granitic, and quartzitic pebbles in a mostly arkosic matrix.

**The Cobalt Group** is subdivided into Gowganda and Lorrain Formations.

The Gowganda Formation, which lies conformably on the Serpent Formation and dips 10° to 55°NE, (Dressler, 1982), comprises sandstone interbedded with wacke, arkose, and minor conglomerate. The units are widely exposed from Scadding Bay to Parkin Township, surrounding Lake Wanapitei from east to northwest. The sediments originated from the erosion of granitic rocks in the Cobalt area northeast of Lake Wanapitei, approximately 2500 to 2155 Ma ago (Van Schmus, 1965, p.755; Fairbairn et al., 1969, p.489). The main constituents of the sandstone are quartz, plagioclase, K-feldspar, chlorite, and matrix of similar composition plus opaque minerals. The transformation into arkose and wacke is characterized by an enrichment in lithic clasts and feldspar, with depletion in quartz content. Minor conglomerates form the lower part of the sedimentary sequence (Dressler, 1984). They contain poorly sorted fragments of granite, gabbro, metasediments, metavolcanic rocks, and quartzite set in a greywacke matrix.

The Gowganda rocks originated in a transitional environment between glacial and marine conditions. Glaciation was the main process of sediment transportation and deposition. Slumping and turbidity currents played minor role (Dressler, 1982). The formation has been recognized as one of the possible target rocks for the Wanapitei meteorite impact event (Dence and Popelar, 1972). Many fragments of unshocked quartzitic sediments from Pleistocene glacial float, south of the lake, are mineralogically and chemically similar to the Gowganda sandstones.

The Lorrain Formation is composed of sandstone, arkose, and wacke. The rocks outcrop in the north and northeastern margin of the lake, north of the Gowganda deposits and southeast of the Portage Bay (Figure 1). The oldest unit is wacke, which grades upward into arkose. Toward the top of the formation, the arkose loses feldspathic content by replacing it with sericitic matrix and becoming a quartz arenite, the most abundant unit closing the cycle of sedimentation.

**Nipissing Intrusive rocks** cut through the Huronian Supergroup and older rocks (Figure 1). In the Lake Wanapitei area, the main lithologies are gabbro and minor granodiorite, granite, quartz-plagioclase porphyry, and pegmatite (Dressler, 1982). The northwesterly oriented sills and dikes are controlled by faults

and joints. The biggest intrusion is known as the Lake Wanapitei Nipissing Gabbro Intrusion and is located east of the Lake Wanapitei (Figure 1). Dikes and sills are dispersed throughout the entire area, except for the northeastern margin of the Lake Wanapitei. Gabbros display a variety of textures from subophitic to equigranular and pegmatitic types. The upper parts of the gabbroic intrusions often consist of granophyre and minor granodiorite. The largest occurrences of this type are known from the Crystal Gold Mine (Portage Bay), and central Matagamasi Lake (Dressler, 1982).

The Nipissing Intrusive rocks display hydrothermal mineralization. Coarse quartz, quartz-carbonate, and carbonate veins are common in the gabbros; however, their relationship to the Nipissing Intrusives is not clear. The veins seem to have originated from remobilization of carbonate minerals of the Espanola Formation during emplacement of the Nipissing gabbro intrusions (Dressler, 1982). The Lake Wanapitei Nipissing Gabbro Intrusion contains gold bearing hydrothermal quartz and quartz-carbonate veins, attracting mineral exploration in the area. The veins are located in the upper part of the intrusion. The base is enriched in Cu, Ni, Co, and minor concentrations of other metals. The structure, composition, and location of the mineralized zones are regarded normal for this type of intrusions (Dressler, 1982). The Nipissing intrusions may also be potential target rocks for the Lake Wanapitei impact (Dence

and Popelar, 1972; Winzer, 1975; Wolf et al., 1980).

In the west, the Lake Wanapitei borders on the norites and gabbros of the Sudbury Igneous Complex. It is beyond the scope of this work to discuss the Sudbury Structure and the voluminous literature on the subject, which was reviewed in Pye et al. (1984).

Middle Proterozoic mafic intrusive rocks (Figure 1) are the youngest Precambrian units in the area and are represented by dikes of olivine diabase. The dikes were emplaced 1460 ±130 Ma ago (Gates et al., 1973). However, divided opinions exist on this matter (Dressler, 1982). The thin, northwesterly elongated dikes were produced by long term regional stresses that emplaced the Sudbury Swarm (Dressler, 1982).

## Quaternary

Quaternary sediments in the Lake Wanapitei area directly overlie the Precambrian rocks. They are mostly Pleistocene glacial till, fluvioglacial sand and gravel deposits, and Recent swamp, lake, and stream deposits (Dressler, 1982). Pleistocene glaciers advanced several times over the area, extensively eroding the bedrock. The last, Wisconsinian glaciation, is the only one known from the deposits. The largest moraine deposits occur immediately south of the Lake Wanapitei (Plate I). The glacial striae found at several locations in the area point in the

southwestern direction (Dressler, 1982) of glacial transportation and deposition. Glacial and fluvioglacial deposits range from well sorted sands to gravel with pebbles and boulders with a considerable clay content. The pebbles and boulders represent mixed fragments of shocked, post impact material and country rocks some of which may have been scoured from the Wanapitei crater floor. The northern part of the Lake Wanapitei area is dominated by glaciofluvial outwash deposits of fine, well sorted, thick sands with minor gravel and till.

## The Wanapitei Impact Rocks

The rocks from Wanapitei Lake studied in this work are samples from the collections of Geological Survey of Canada, the Ontario Geological Survey, and those collected by the author. Ninety three thin sections were examined. The rocks are placed in groups of similar grade of shock metamorphism. The description of twelve samples collected by the author is included in Appendix A.

Generally, based upon macro- and microscopic observations, the Wanapitei impact rocks fall into the five main lithological types:

**I. Polymict breccias**

**II. Moderately shocked granitic gneiss**

**III. Shocked sediments with glass**

**IV. Suevite breccias**

**V. Vesicular glassy melt rocks**

The groups are listed according to increasing grade of shock metamorphism. Glass is present in rocks of all of the groups occurring as clear glass, brown glass or both, showing mixing. **Polymict breccias** are represented by a variety of multi-rock type breccias with a signature of weak to moderate degree of shock metamorphism (Chao, 1968). The rocks are light grey to

brown. Generally, the breccias contain lithic and mineral fragments and minor glass set in fine fragmental matrix.

The lithic clasts are dominated by varieties of sandstone, arkose, and wacke. Other, minor rock types present, include diabase, gabbro, and gneiss. Mineral fragments reflect the lithic clasts. The main constituents are quartz, feldspar, minor mica, pyroxene, amphibole, and opaque minerals.

The matrix is usually fine, fragmental, and in some cases partly glassy. The proportion of glass in the breccias does not exceed 15% of the matrix. The glass can be clear, brown, or mixed. Vesicles, if present, may display elongation resulting from flow.

Sub-solidus shock metamorphism in these rocks is represented by minor quartz with planar features. The shocked quartz with planar features accounts for up to 5% of the volume of quartz in clasts. The planar features are nondecorated and poorly visible. Those observed were c-{0001} and $\omega$-{10$\bar{1}$3} type A and B respectively in up to three sets per grain, indicating a low to moderate grade of shock metamorphism with pressures of <10-12 GPa (Robertson and Grieve, 1977; Stöffler, 1972). Other mineral deformations include kinking in crystals of pyroxene, amphibole, and plagioclase, and irregular fracturing. The largest variations among the rocks of this group occur with respect to the content of glasses, the presence of planar features in quartz, and variety of lithic fragments present in the rocks.

The group is represented by sample WTB-2-2U described in Appendix A and shown in Plate III.

**Moderately shocked granitic gneiss** can be found in the Pleistocene till as pebbles and boulders up to 50 cm in diameter and as lithic fragments in shocked breccias reaching up to several cm in diameter. The rock displays characteristic gneissic texture. The granitic composition of gneiss is variable with respect to proportions of the main constituents. Quartz ranges between 35 and 75% of the mode, feldspars range between 10 and 35%, mafic minerals reach up to 25%. The mafic constituents are pyroxene and amphibole. However, due to strong alteration they are difficult to recognize. Minor minerals such as chlorite, muscovite, and opaque minerals account for < 1-2% of the mode. Chlorite and muscovite are products of alteration of the main constituents (e.g., sericitization of plagioclase). Shock metamorphism in these rocks is expressed by kinking of twin lamellae in plagioclase, planar features in quartz, and interstitial glass. Some gneisses display only kinking (especially those forming lithic clasts in breccias). The stronger shocked units contain all of the deformation indicators. Quartz with planar features accounts for up to 50% of total quartz content. Planar features in quartz are nondecorated to "moderately" decorated, usually forming one set per grain. However, in places ~25% of shocked quartz can have

two or three sets per grain. The dominant lamellae are $\omega$-{10$\bar{1}$3} type-B, minor $\pi$-{10$\bar{1}$2} type-D, and s-{11$\bar{2}$1} type-D, which indicate shock pressures of ~12-38 GPa (Robertson et al., 1968; Robertson and Grieve, 1977; Stöffler, 1972). The interstitial glass is strikingly concentrated around mafic minerals. The glass accounts for no more than 10% of the mode. It is completely absent in gneisses with low mafic content. The glass is brownish, in places displaying incipient crystallization of pyroxene. Neither vesicles nor flow textures were observed. The characteristic "mafic-close" interstitial concentration of the glass suggests that the shock metamorphism in these rocks reached only the initial stage. The glassy phase developed later due to waste heat, which caused thermal annealing of the rocks. The group is represented by sample MSWX-119-70 described in Appendix A.

**Shocked sediments with glass** represent rocks of low density (caused by vesiculation). The main constituents are the "host" sediment and interstitial vesicular glass. The sediments are mostly quartzite, arenite, wacke, and arkose. Quartz and feldspars in these rocks are moderately to intensely fractured and partly converted into diaplectic glass (up to 15% of the volume). The interstitial glass is dominantly brown, with irregular vesicles (in shape, size, and distribution). The colouring of the interstitial glass follows changes in

composition of the "host" rock; the less mafic content of sediment, the lighter the glass. The presence of the diaplectic glass sets the maximum conditions of sub-solidus shock metamorphism of rocks of this group at peak pressures of approximately 30-50 GPa (Stöffler, 1972). The same range of pressures can be ascribed to formation of coesite (Stöffler, 1972); this mineral was observed in glassy quartzitic sediments as minute inclusions in a brown coloured glass (Dence and Popelar, 1972), but was not encountered by the writer. It appears that the rocks of this group underwent moderate to strong shock metamorphism with high strain-rate sub-solidus effects combined with high temperatures of approximately 2000°C (Chao, 1968). The group is represented by sample WTB-2-2F described in Appendix A and shown in Plate IV.

**Suevite breccia** is the least abundant rock type observed among the five groups of impact lithologies. By definition, they are breccias containing a variety of shock metamorphosed rock fragments. The rocks are distinguished from volcanic analogues, such as tuff breccia, by shock metamorphic effects (Gary et al., 1973).

Suevites from the Wanapitei structure are characterized by large (up to several cm in diameter) inclusions of glassy and lithic fragments in a light coloured fragmental matrix. The rocks are

extensively fractured and break apart with ease. The glassy fragments account for up to 50% of the mode. They are mostly subrounded, though angular varieties were also observed. The glass can be colourless, brown, or can be both, intermixed and forming flow textures. The index of refraction of the glasses is approximately 1.46 (Dence and Popelar, 1972, p.120; P.B. Robertson, personal communication), with higher values for the brown type. Vesicles are present in both types of glasses. However, the brown glass usually has a higher content (max. 50% of the mode in brown vs. 25% in colourless type). The shape of the vesicles varies from rounded to oval and irregularly elongated or sinuously bent, sometimes filled partially or entirely with recrystallized silica. Lithic fragments recognized are sandstones, siltstones, argillites, wacke, gabbro, and diabase. Their concentration is variable and reaches up to 35% of the mode. The lithic fragments are often brecciated into single mineral grains (up to 10% of the mode), dominated by quartz. Planar features are present in about 2.5% of the quartz grains. The deformations (after Robertson et al., 1968 and Robertson and Grieve, 1977) represented by $\omega$-$\{10\bar{1}3\}$ type-B, m-$\{10\bar{1}0\}$ type-C, and $\pi$-$\{10\bar{1}2\}$ type-D features with shock pressures of ~12-38 GPa (Stöffler, 1972), forming up to three sets per grain. Other, sub-solidus shock metamorphic effects include maskelynite (diaplectic glass of plagioclase composition; Tschermak, 1872) formed at shock pressures of 30-45 GPa

(Stöffler, 1972), and twin kinking in feldspars and mafic minerals.

The suevite breccias are represented by sample WTB-3S-90 described in Appendix A and shown in Plate V.

**Vesicular glassy melt rocks** generally contain a matrix of vesicular glass with inclusions of quartz, feldspars, and minor amounts of mafic and opaque minerals.

In thin section, the glass is seen to consist of two types. The most abundant is clear, homogeneous glass with perlitic cracks, vesicles, and refractive index between ~1.45 and ~1.47. The second type is vesicular brown glass, averaging a higher refractive index of >1.50 (Dence and Popelar, 1972; P.B. Robertson, personal communication), and often displaying flow textures. In places, both glasses intermix, displaying vesicles, flow textures, and perlitic cracks. The vesicles range from less than 0.01 mm to several cm in diameter, displaying partial or entire filling with microcrystalline silica. Their shape can be spherical, oval, or irregular with strong elongation. Abundance of the vesicles changes from about 3% in clear glasses to 15% in brown and mixed types. Quartz inclusions can make up to 25% of the mode. The main types of quartz are irregularly fractured grains, ballen quartz, and quartz with planar features. The ballen quartz (the annealing product after diaplectic quartz glass; Müller and Hornemann, 1969) accounts for approx. 50% of

the total quartz content. It displays mosaics of characteristic semicircular cracks (Plate VI) and minor concentrations of diaplectic glass. Quartz with planar features accounts for up to 2.5% of the total quartz. The planar features are decorated or nondecorated and represented by minor c-{0001} type-A, $\omega$-{10$\bar{1}$3} type-B, $\xi$-{11$\bar{2}$2} type-C, $\pi$-{10$\bar{1}$2} and s-{11$\bar{2}$1} type-D deformations (Robertson et al., 1968; Robertson and Grieve, 1977), forming up to three sets per grain. Quartz inclusions are usually subrounded to rounded, some strongly embayed with individual embayments reaching 1.5 mm in diameter. Quartz can be also observed in clusters of grains making up to 5% of the mode. Much less common, but distinct, is a type of quartzitic material, which appears as rosettes of elongated crystals devitrified from matrix glass. This type of quartzitic crystallization is usually associated with highly vesicular clear glasses, where the rosettes of silica can make up to 75% of the mode.

Feldspar is represented by the incipient crystallization of plagioclase of two distinct size populations in the matrix. Finer laths average 0.05 mm; whereas, the coarser blade-like crystals reach up to 1.0 mm. Both types coexist in varying proportions. The finer plagioclase accounts for up to 15% of the mode, the coarser for up to 5%. Larger blade-like crystals often form radial or variolitic aggregates (Plate VII). Minor phases in these rocks are opaque minerals, mostly pyrite, which are

concentrated in lamina-type zones (Plate VIII, lower right). The grade of shock metamorphism in rocks of this group is the highest among the Wanapitei samples. Lechatelierite, the high pressure polymorph of quartz,was observed as curvilinear inclusions in a glassy matrix (Dence and Popelar, 1972). The peak pressures and temperatures of shock metamorphism of rocks of this group can be estimated from the conditions of formation of this mineral. Lechatelierite crystallizes from liquid silica formed at pressures of 50-65+ GPa and temperatures of ~1600-2500°C (Chao, 1968; Stöffler, 1972).

The group is represented by samples WTB-2T-90, WTB-2-2RA, WTB-2-2C, WTB-2A-2F, WTB-2-2G, WTB-2-2X, WTB-2A-2E, WTB-2-2M described in Appendix A and shown on Plates VI, VII, VIII, IX, X, XI, XII and XIII, respectively.

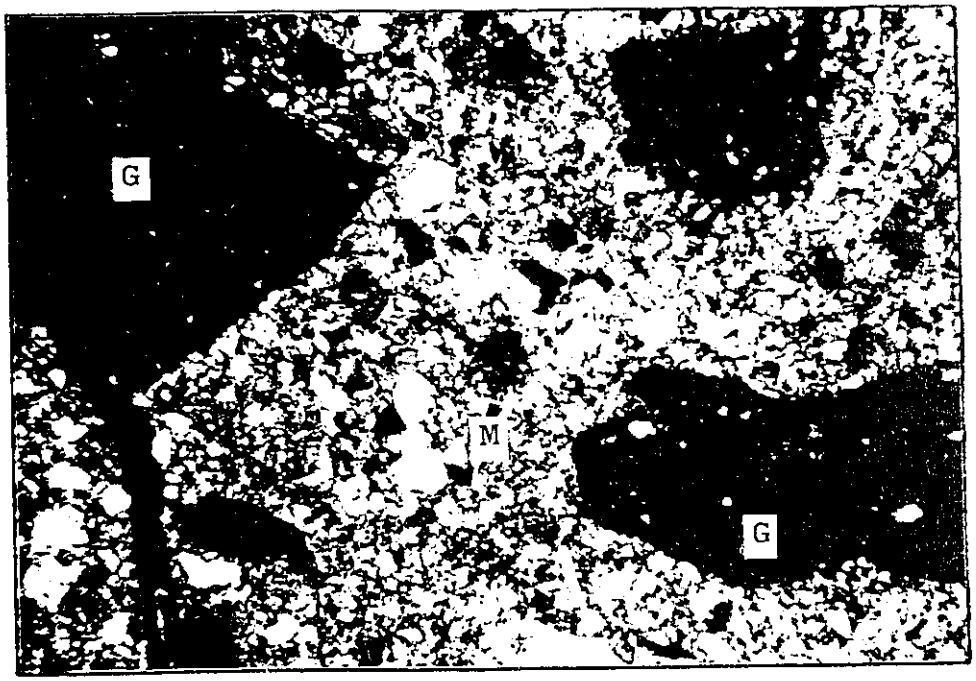


Plate III. Sample WTB-2-2U. Polymict glassy breccia, Lake Wanapitei. Large glassy fragments (G) in fragmental matrix (M) with lithic and mineral clasts. Crossed polarized light (CPL), field of view 4.6x7.0mm.

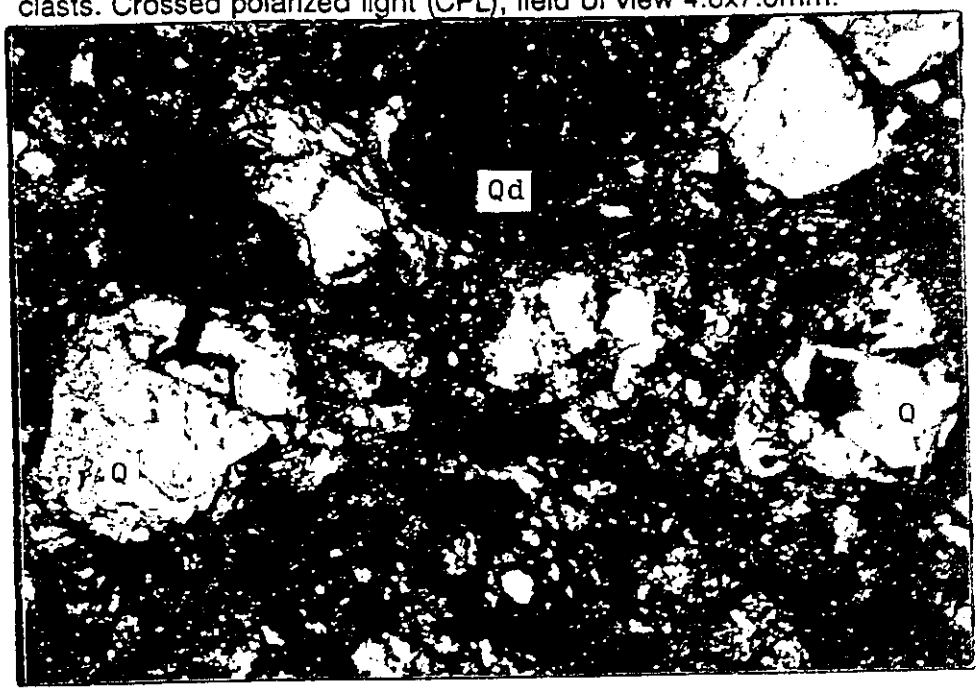


Plate IV. Sample WTB-2-2F. Shocked quartzitic sediment with glass, Lake Wanapitei. Strongly fractured quartz (Q) surrounded by fused glass. Quartz grains are partially or entirely converted into diaplectic glass (Qd). CPL, field of view 2.3x3.5mm.

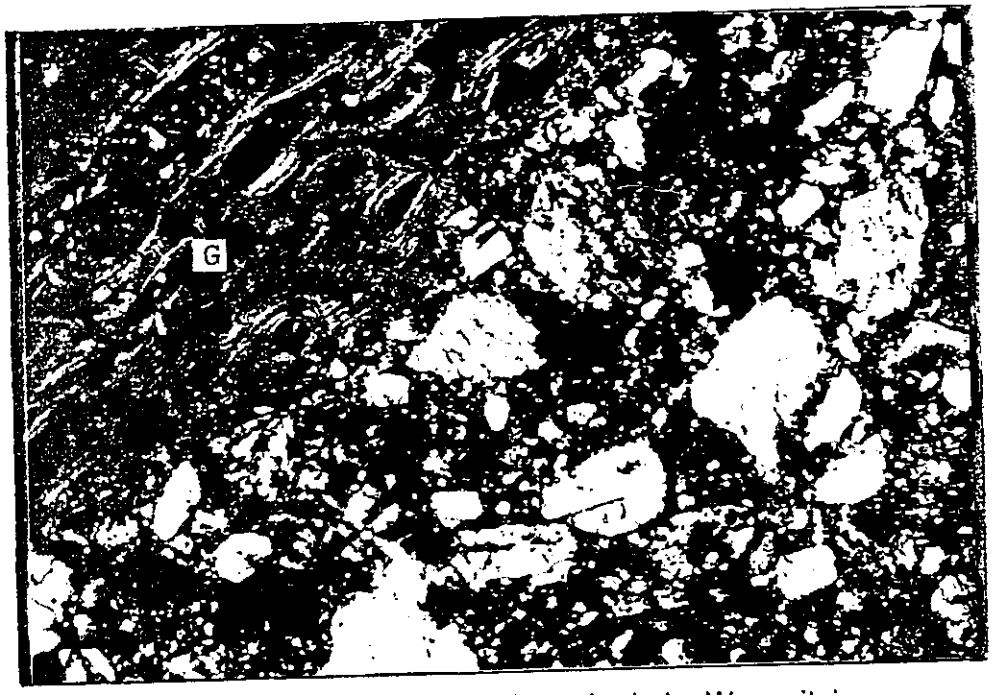


Plate V. Sample WTB-3S-90. Suevite breccia, Lake Wanapitei. Large glassy fragments (G) and detritic material including quartz with planar features and lithic clasts set in glassy matrix. CPL, field of view 0.9x1.4mm.

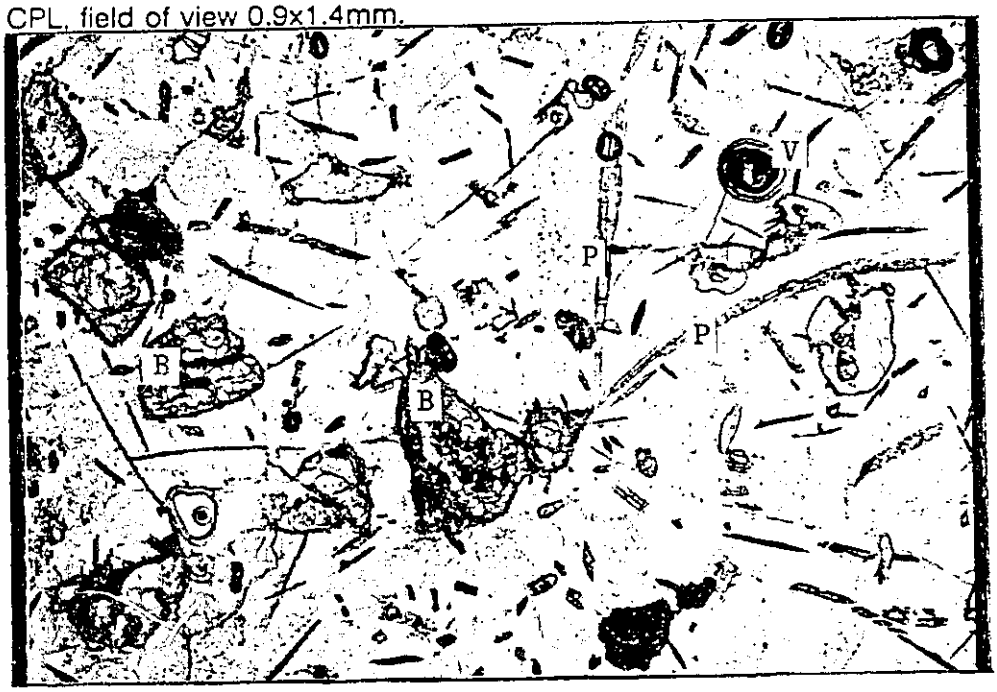


Plate VI. Sample WTB-2T-90. Vesicular glassy melt rock, Lake Wanapitei. Ballen quartz (B), "blades" of plagioclase (P), and rounded vesicles (V) are set in colourless glass with perlitic cracks. Plain Polarized Light (PPL), field of view 2.3x3.5mm.

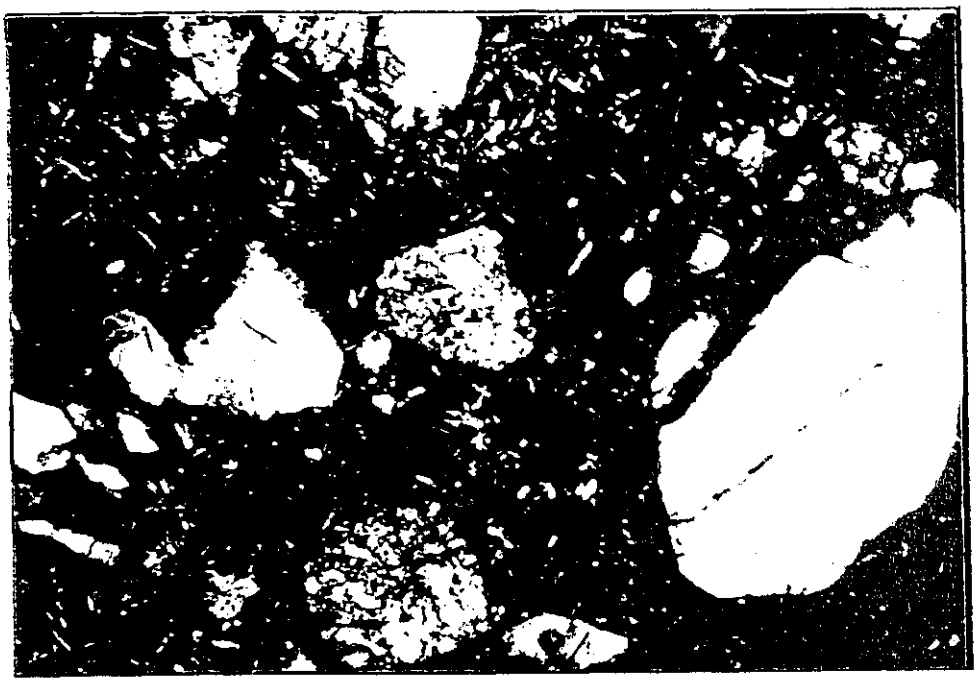

Plate VII. Sample WTB-2-2RA. Vesicular glassy melt rock, Lake Wanapitei. Inclusions of fractured and ballen quartz set in glassy matrix partially crystallized to plagioclase. CPL, field of view 0.9x1.4mm.


Plate VIII. Sample WTB-2-2C. Vesicular glassy melt rock, Lake Wanapitei. Shocked quartz with one set of planar features (SQ) in glass with perlitic cracks, minor feldspars, and opaque minerals (OPq). PPL, field of view 0.9x1.4mm.

Plate IX. Sample WTB-2A-2F. Vesicular glassy melt rock, Lake Wanapitei. Shocked quartz with planar features set in matrix of mixed glasses with flow texture. PPL, field of view 0.9x1.4mm.

Plate X. Sample WTB-2-2G. Vesicular glassy melt rock, Lake Wanapitei. Large vesicle with mineral and lithic clasts surrounded by thin devitrified zone; all set in colourless glass with lithic fragments and quartz inclusions. CPL, field of view 4.6x7.0mm.


Plate XI. Sample WTB-2-2X. Vesicular glassy melt rock, Lake Wanapitei. Inclusions of ballen quartz in glass with perlitic cracks and spherical vesicles (V) with devitrified "collars". CPL, field of view 0.9x1.4mm.


Plate XII. Sample WTB-2A-2E. Vesicular glassy melt rock, Lake Wanapitei. radially growing quench feldspars (centre) and variolitic assemblage (Vr) in colourless glass with inclusions of ballen quartz. CPL, field of view 2.3x3.5mm.

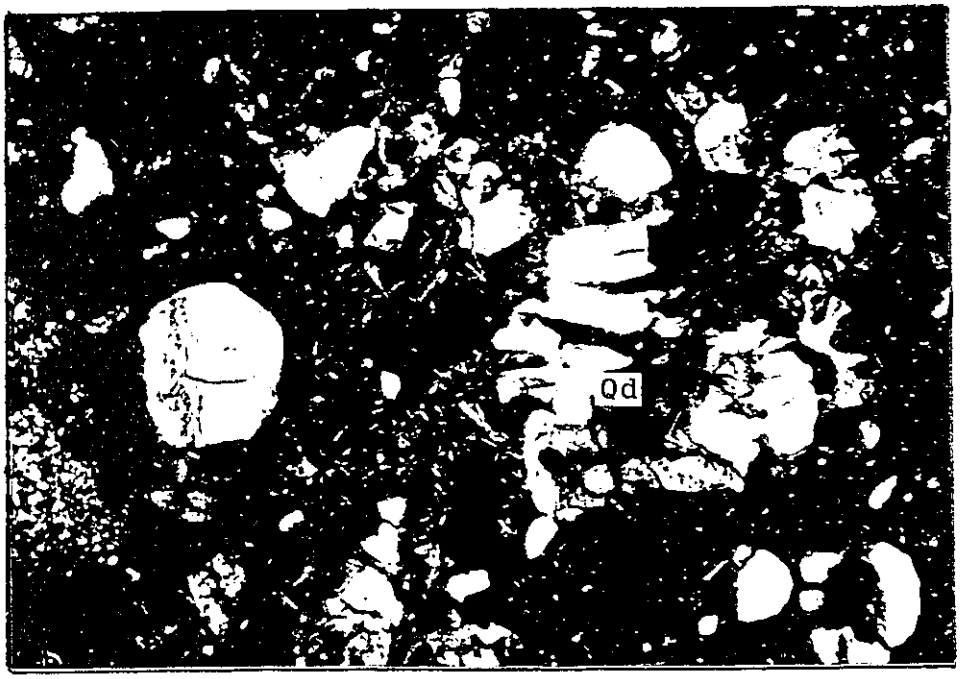


Plate XIII. Sample WTB-2-2M. Vesicular glassy melt rock, Lake Wanapitei. Partly diaplectic cluster of quartz inclusions (Qd) set in vesicular glass with fine inclusions of quartz and feldspars. CPL, field of view 2.3x3.5mm.

## Temperature and Pressure Conditions of the Impact

The maximum temperature and pressure generated during an impact depend upon projectile and target rock type and impact velocity. The sudden rise of pressures and temperatures to extremely high levels, followed by quenching, in a very short time, result in metastable and non-homogeneous phases (e.g. glass). The unique way in which this ultra-rapid geological process develops produces characteristic sets of plastic and brittle transformations. Some of them, such as those that produce fused and diaplectic glasses, high pressure polymorphs, planar features, geophysical anomalies, or characteristic tectonic discontinuities in the area, may survive as the only evidence of an impact, long after erosion has destroyed the original crater form.

The range of pressures and temperatures created by the Wanapitei impact event can be estimated from the shock metamorphic features recorded in the crater lithologies. These include:

- quartz with fracturing, mineral kinking, quartz with planar elements, diaplectic quartz glass, mosaics of ballen quartz
- maskelynite (Dence et al., 1974).
- coesite (Dence et al., 1974)
- lechatelierite (Dence and Popelar, 1972)
- vesicular fused impact glasses

According to Stöffler (1972), with increasing values of pressure

and temperature, shock metamorphism occurs in stages marked by characteristic deformations. Figure 4 presents the development of the pressure-driven sequence of the shock deformations in the Wanapitei rocks.

Following is the description of the examined deformations, with emphasis on shocked quartz which, however, may not represent the whole suite of shock features present in the Wanapitei structure.

The weakest deformation, **fracturing**, is present in most minerals in the observed samples. It forms rare to very dense irregular patterns. Less abundant **mineral kinking** appears in feldspars and sheet-silicates. However, the fractures and kinking neither identify, nor characterize the shock metamorphism conditions. However, their abundance, as in the Wanapitei samples, indicates extensive deformation of the rocks. The conditions necessary for their occurrence do not exceed pressures of 15 GPa and temperatures of 100°C. To date, no shatter cones from the Wanapitei impact site have been found. Those reported from the southern margin of the lake (Dressler, 1982), were later ascribed to the Sudbury Structure (Ogilvie et al., 1984).

Figure 4. Schematic presentation of residual shock effects produced within specific pressure ranges in the quartzitic material from the Lake Wanapitei impact structure (adapted from Stöffler, 1972).

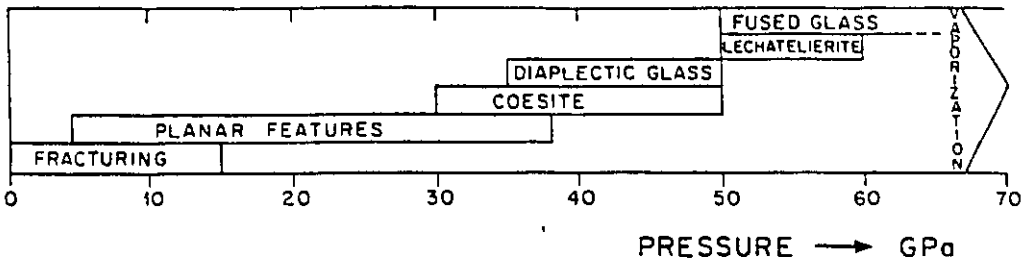


Figure 5. Planar features in quartz from the Lake Wanapitei impact structure (This work).

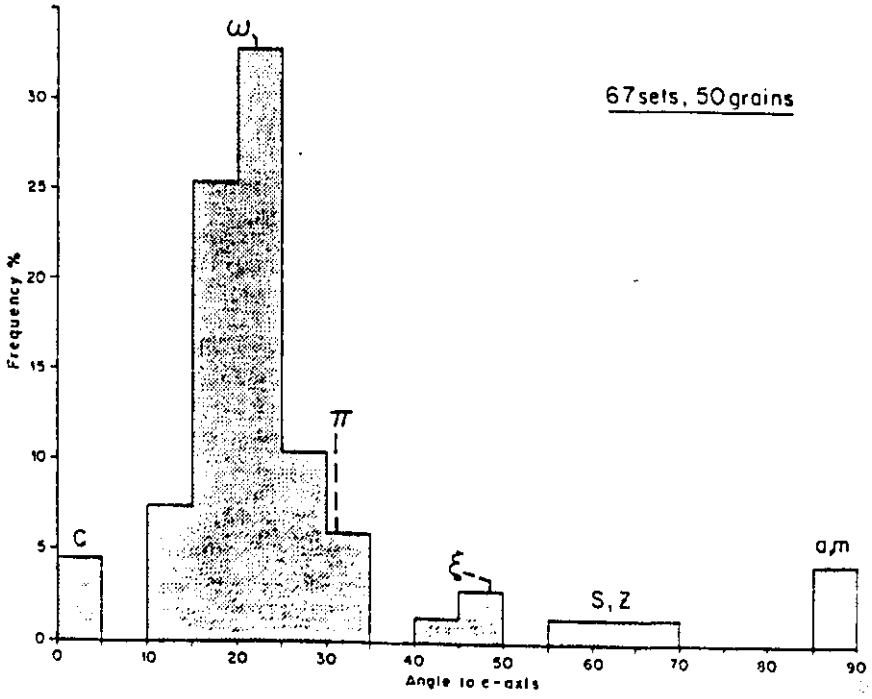

**Planar features in quartz** are not abundant. They represent plastic deformations in crystals produced by gliding along discrete crystallographic planes under shock pressures exceeding the so-called Hugoniot elastic limit of quartz, HEL (Stöffler, 1972). The definition of the HEL is "..the maximum normal stress that the material may withstand under one-dimensional compression, without internal rearrangement (such as plastic flow or brittle fracture) taking place at the shock wave front" (Ahrens and Rosenberg, 1968). For quartz, the HEL occurs at pressures of 4.5-14.5 GPa, depending upon the crystal orientation (Duvall and Graham, 1977). The observed sets of the planar deformations in quartz were mostly ω-{$10\bar{1}3$} accompanied by sets of π-{$10\bar{1}2$}, a-{$11\bar{2}0$}, s-{$11\bar{2}1$}, ξ-{$11\bar{2}2$}, c-{0001}, z-{$01\bar{1}1$}, and m-{$10\bar{1}0$} (Plate VIII and IX). The nomenclature of the crystallographic planes is as follows:

{$10\bar{1}3$}-rhombohedra (ω)

{$10\bar{1}2$}-rhombohedra (π)

{$11\bar{2}0$}-second order prism (a)

{$11\bar{2}1$}-second order trigonal dypyramid (s)

{$11\bar{2}2$}-second order trigonal pyramid (ξ)

{0001}-basal pinacoid (c)

{$01\bar{1}1$}-negative rhombohedra (z)

{$10\bar{1}0$}-unit prism (m)

The classification of the Wanapitei planar features as C-type and D-type is based on the criteria given by Robertson et al.

(1968) and Robertson and Grieve (1977). The frequency of the features versus angles to the c-axis of the crystals is presented in Figure 5. Many of the features are decorated and form up to three sets per grain. Their formation occurred at pressures between 4.5 and 38 GPa (Stöffler, 1972, p.280).

**Stishovite** was not observed in the shocked rock samples from Lake Wanapitei. This high pressure polymorph of $SiO_2$ is known from the Barringer crater in Arizona, and the Ries crater in Germany (Bunch, 1968). Stishovite forms at pressures of 12-45 GPa during shock compression (Stöffler, 1971, p.5475). Often it is associated with planar features in quartz, "decorating" them as series of minute inclusions. In the Wanapitei impact glasses, with a refractive index of approximately 1.46, the mineral could account for up to 0.005% of the primary quartz (Stöffler, 1971, p.5483). Thus, its identification would be difficult. Nevertheless, several features of the Wanapitei crater lithologies suggest the possibility of its presence, or at least the conditions suitable for its formation:

1. The presence of quartz with decorated planar features.
2. The association of coesite with stishovite is well known from the impact craters at Ries, Germany, and in Barringer, Arizona.
3. The pressures and temperatures generated by the Wanapitei impact were sufficient to produce stishovite (Dence and Popelar, 1972; This work). Above 600°C (at 1 atm. pressure) stishovite

becomes unstable (Chao, 1968, p.149), but, nonuniform distribution of pressure and temperature in the dynamic environment of the crater could result in partial, localized preservation of the mineral.

4. The high volume of fused glasses relative to sub-solidus shocked quartz suggest a high degree of shock metamorphism and the possibility that any stishovite, formed during shock compression, would have changed into an amorphous silica under conditions of shock release.

**Coesite** from the Wanapitei shocked rocks that occurs as minute inclusions in brown glasses, has been described by Dence and Popelar (1972). Generally, coesite may form either by meteoritic impact, or by high grade regional metamorphism. Non-impact generated coesite has been reported in xenoliths from kimberlites of Roberts Victor Mine, Republic of South Africa (Smyth and Hatton, 1977), high-pressure metasediments in the Alps (Chopin, 1984), coesite-eclogites in the Norwegian Caledonides (Smith, 1988), quartz pseudomorphs from eclogites in the southern Urals and Münchberg, Germany (Chesnokov and Popov, 1965), and from eclogites in Shandong province in east China (Enami and Zang, 1990). The non-impact coesite has been estimated to be stable at pressures between 2.9 and 8 GPa, and at temperatures around 800°C (Mirwald and Massonne, 1980, p.469). The environment suitable for crystallization of coesite

is long-term exposure to steady or steadily rising pressures and temperatures at depths exceeding 90 km (Schulze and Helmstaedt, 1988, p.440; Enami and Zang, 1990, p.381).

On the other hand, the impact-generated metastable coesite requires pressures of 30 to 50 GPa and temperatures between 380 and 1000°C (Stöffler, 1972, p.98; Chao, 1968, p.138). The characteristic feature of shock processes is a very short time during which the peak conditions are reached and maintained. The coesite forms during the release of the shock compression, behind the shock front (Stöffler, 1971, p.5474). The duration of such conditions and the whole time of shock transition influence crystallization of metastable phases, such as the coesite. The longer the duration of the extreme pressure and temperature yields better crystallization (Stöffler, 1972). The non-impact coesite, which crystallizes during a long-term stable conditions, forms crystals which are relatively easily identifiable under the microscope. In contrast, the very rapid restructuring of $SiO_2$ caused by an impact produces minute inclusions of coesite, hardly recognizable in thin sections. This is the case for the coesite from Wanapitei, which is of shock origin. There is no evidence of rocks originating from depths of 90 km in this area.

**Lechatelierite** was found in Wanapitei impact melt rocks by Dence

and Popelar (1972). This form of fused $SiO_2$ can appear in a silica melt with reduced viscosity, forming the observed elongated, curvilinear inclusions. Lechatelierite is the highest pressure fibrous variety of amorphous $SiO_2$, which forms from liquid silica at pressures of above 50-65 GPa, and temperatures of ~1600-2500°C (Chao, 1968, p.138). Lechatelierite in association with coesite and stishovite is known to have survived in such craters as Barringer, Kentland, and Ries.

**Diaplectic glasses** of quartz, commonly present in the Wanapitei impact melt rocks (Plate IV), usually form under pressure of 35 to ~50 GPa (Stöffler, 1972). The upper limit of pressure is determined by the peak of the post shock temperature. To remain diaplectic, the temperature cannot exceed the melting point of quartz (Stöffler, 1972, p.98). The diaplectic glasses are the reversion product of high-pressure phases formed during shock compression. The high-pressure phases react to the pressure release by transformation to a phase of low density, i.e. diaplectic glass, without melting (Stöffler, 1972). It seems that in the observed Wanapitei impact melt rock, some of the diaplectic glass recrystallized into ballen quartz due to the heat of the melt matrix. Maskelynite (diaplectic glass of plagioclase), a minor phase observed in the Wanapitei samples (Dence and Popelar, 1972), forms within the similar range of pressures, following the same pattern of formation as quartz

(Stöffler, 1972).

**Fused glasses** from Wanapitei were compared with melt glasses from the Ries crater, Germany, because of their similarity of refractive indices, oscillating around 1.46 (Dence et al., 1974, p.121). The peak pressures of >50 GPa can be estimated for the Wanapitei material (Stöffler, 1972). Theoretically, melting of quartzitic material occurs at pressures between ~50 and 65 GPa and temperatures reaching up to 2500°C, when the rock starts to vaporize (Melosh, 1989, p.41). Based on the static model of shock metamorphism zones and associated transformations of silica material in the Ries crater (Stöffler, 1971), it appears that the Wanapitei event could cause rocks to vaporize from an area of approximately 2.5 km in diameter. For the quartzitic melt, the temperature of vaporization would have to reach at least 2500°C under pressures of at least 70 GPa (Chao, 1968, p.138).

The presence of fused glasses with flow textures suggest that high temperatures from the post-impact waste heat were sufficient to sustain the flow of the melts for some time after the event. Presumably, the silica-rich melt derived largely from the quartzitic Huronian sediments increased in viscosity fairly fast during cooling. Thus, the observed fused glasses with flow textures were in motion for only a very short time before settling. The strikingly spherical vesicles in some of those glasses indicate degassing, which occurred just after the melts

ceased movement. Probably, the formation of lechatelierite in the melts took place at the same time. The fresh state of preservation of the Wanapitei glasses reflects their relatively young age of 37 Ma (Winzer et al., 1976). A large number of perlitic cracks, quench plagioclases, and common tension cracks in quartz indicate a relatively rapid drop in temperature during cooling of the melts, when the temperature conditions of the surroundings influenced the local, post impact environment within the crater. Unfortunately, the floor of the crater has been eroded by glacial action, and the primary distribution of the shocked rocks can only be approximated from the grade of shock metamorphism recorded in the recovered target rocks. The shocked samples recovered from the glacial float represent a fraction of the post impact lithological varieties in the crater.

Another difficulty in estimating the maximum pressures and temperatures during the shock wave propagation and after the shock was relieved, is the possibility of secondary thermal annealing after burying shocked rocks underneath the hot layers of impact breccia. This could obliterate the primary evidence of original impact conditions (Stöffler, 1972). Thus, for example coesite and stishovite, if ever formed, could revert to more stable phases. The evident abundance of ballen quartz and fused impact glasses signal such process. In general, several features of the Wanapitei event, such as presence of the planar

deformations in quartz, diaplectic quartz glasses and the fused silica glasses, presence of coesite and lechatelierite set the peak conditions of Wanapitei impact event at pressures of **at least 65-70 GPa** (the maximum pressure was probably much higher) and peak post shock temperatures in the range of 2000-2500°C. Figure 6 illustrates schematically the distribution of zones of shock metamorphism in the Wanapitei structure. Similar concepts of shock conditions have been proposed for the Ries crater, Germany (Stöffler, 1966 and 1971; Engelhardt and Stöffler, 1968), for the Sudbury structure, Ontario (Lakomy, 1990b), and for the Manicouagan structure, Quebec (Dressler, 1990). Analogous to the role of shocked plagioclase at the Manicouagan structure (Dressler, 1990), the continuous progress of shock deformations recorded in quartz from Wanapitei serves as guide through distribution of shock pressures in the presented model (Figure 6). The sequence of pressure-dependent shock deformation zones (Figure 6) is modified from the accounts given by Stöffler (1971), Engelhardt and Stöffler (1968), Dressler (1990) and Lakomy (1990a&b). According to Lakomy (1990a), the size of apparent and transient crater (the initial cavity formed by the cratering flow field, Dence et al., 1977), can be estimated from the maximum radial distribution of shock features. The procedure, however, can be applied to the structures, in which the basement geology is readily accessible, enabling recognition of distribution of shock features. In the case of the Wanapitei

structure, remnants of the crater are submerged, and most of the impact lithologies have been eroded and relocated by glacial processes. In these circumstances, the distribution of shock features was estimated from the size of the apparent crater (8.5 km in diameter, Dence and Popelar, 1972), based on the gravity anomaly.

The transient cavity at Wanapitei measured ~4.9 km in diameter. It was calculated from the formula: $D_t=0.57xD_a$ ($D_t$-transient crater diameter, $D_a$-apparent crater diameter) given by Lakomy (1990a). The formula applies to complex craters characterized by a central peak. Despite the lack of field confirmation of a central peak at Wanapitei crater, the formula was used mainly because of the size of the structure (8.5 km in diameter), which is larger than many complex craters with a central peak, such as Gow Lake (4 km in diameter), Pilot Lake (5 km in diameter), Lac Couture (8 km in diameter), and Lac la Moinerie (8 km in diameter), Canada. The zones of shock metamorphism from the crater's centre are:

1. Zone of melt and vapour, minimum 70 GPa.
2. Zone of fused glass with minor lechatelierite, ~50-65 GPa.
3. Zone of minor planar features (formed up to ~38 GPa), diaplectic glass, and coesite, ~35-50 GPa.
4. Zone of planar features, coesite, and diaplectic glass (the latter two start appearing at ~35 GPa), ~30-35 GPa.
5. Zone of planar features, ~15-30 GPa.

Figure 6. Conceptual distribution of shock metamorphosed quartz in the Wanapitei impact structure. The model is a schematic adaptation to the parameters of the Lake Wanapitei crater (based on Engelhardt et al., 1968; Stöffler, 1971; Dressler, 1990; Lakomy, 1990a&b).

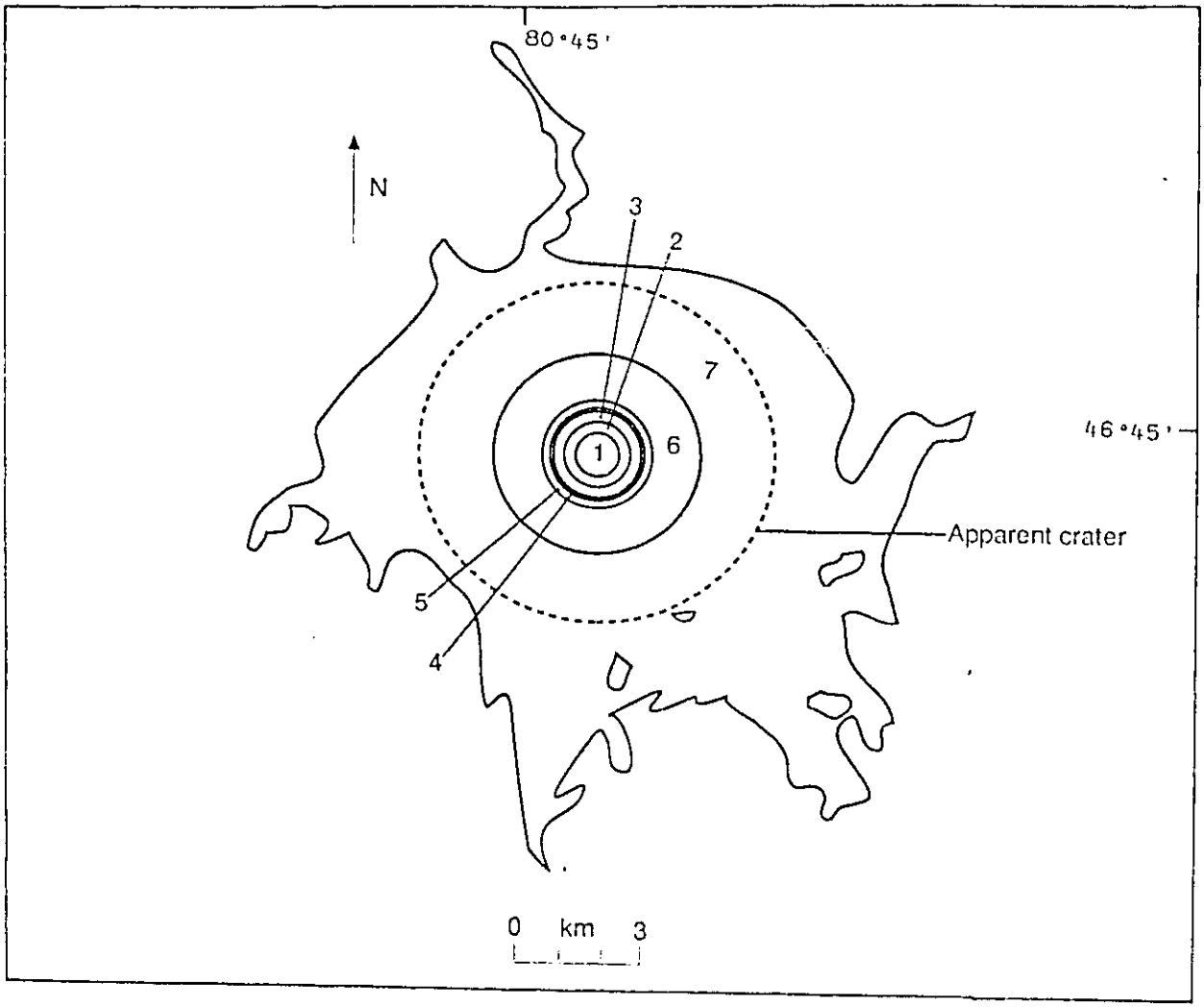


Zones of shock metamorphism:
1. Melt, vapour (min. 70 GPa).
2. Fused glass, lechatelierite (50-65 GPa).
3. Minor planar features*, diaplectic glass, coesite (35-50 GPa).
4. Planar features, coesite**, diaplectic glass** (30-35 GPa).
5. Planar features (15-30 GPa).
6. Kinking, fracturing, planar features (4.5-15 GPa).
7. Fracturing, mineral kinking (<4.5 GPa).

*Appear up to approx. 38 GPa.
**Start appearing at approx. 35 GPa.

6. Zone of mineral kinking, fracturing, and planar features, ~4.5-15 GPa.

7. Zone of fracturing and mineral kinking <~4.5 GPa.

The sequence of shock features listed for each zone reflects their appearance, e.g. in zone 4, planar features can form within the whole range of pressures; thus, there they should be much more abundant than in zone 3, in which they can form only until ~38 GPa. The outer margin of zone 6 defines a transient cavity. The pressures at the margin of zone 6, ~1-2 GPa, are the minimum necessary to produce deformations characteristic of shock processes. The model presented in Figure 6 reveals that five out of seven zones occupy relatively small area of the crater. This suggests, that the rarity of the strongly shocked rocks in the Lake Wanapitei area may not be only due to the erosion and transportation processes, but also due to the initial distribution and range of the shock metamorphism in the crater.

**Geochemistry of the Wanapitei Crater and Target Lithologies.**

The results of the microprobe analyses for major elements of the matrix glasses of vesicular impact melt rocks are presented in Table 1. The smallest difference among the samples is noticeable for the $Al_2O_3$ and $Na_2O$ content. Other constituents display a wide range of concentration levels within the population of samples.

The microprobe results show low values of "totals" for the samples. In author's view, the vaporization of glasses introduced a considerable error to the obtained microprobe readings, resulting in lower "total" values despite the use of defocused beam (to avoid the effect of vaporization) during the analyses. These results are in agreement with analyses obtained previously as listed in Table 1a. The noticeable variation in "totals" can result from different conditions under which the analyses were performed.

As indicated in the previous chapter, glasses observed in the Wanapitei impact melt rocks can be distinguished as clear and brown types. The data for major oxides (Table 1) and the normative calculations (Table 1b) show relatively small differences among the glasses within one-colour group and between the clear and brown types. The difference between the clear and brown glass was analyzed statistically by the t-test, using mean values for each type of glass from Table 1. For 6 degrees of freedom, the t-score obtained was 0.2554, which

indicates (statistically) a lack of significant difference in composition between the two types of glass. The analysis of clear glass from Dence et al. (1974) is different from the other results. A lower content of $SiO_2$ (Table 1a) and consequently quartz (Table 1b) are replaced by a higher concentration of $Al_2O_3$ and feldspars, respectively. This situation results from the composition of the protoliths converted into the glass. This concept seems reasonable in view of the fact that the analysis by Dence et al. (1974) is a mean of four, with very low values for standard deviations ($\leq 0.20$), and according to the authors the analyses "...have been carefully checked by duplicate measurements.." and "...consistent values were obtained.." (Dence et al., 1974, p.120). The glass evidently represents a type of glass formed from more feldspathic protoliths, such as arkose, in contrast to the majority of glasses, which appear to have originated from quartzite (Table 1b). Tables 1c and 1d present the results obtained from samples WTB-2-2X and WTB-2-2C (both are vesicular glassy melt rocks). All targets analyzed were clear glass. The clear glass exists as remarkably homogeneous silica (Table 1c, column 001 and 002; Table 1d, column 001) and inhomogeneous glass with higher content of $Al_2O_3$, $TiO_2$, $Na_2O$, $K_2O$, and FeO (Table 1c and 1d). It reflects the inhomogeneous character of the environment in which the melt rocks formed (R.A.F.Grieve, personal communication). The results of the XRF analyses for the same samples (Table 2) do not reveal

Table 1. Electron microprobe analyses of glasses in impact melt rocks from Lake Wanapitei.

| Sample | Clear Glass | | | | | Mean | Std. Dev. |
|---|---|---|---|---|---|---|---|
| | WTB-2-2X n=8 | WTB-2T-90 n=4 | WTB-2-2C n=8 | WTB-2A-2E n=5 | WTB-2-2RA n=4 | | |
| $SiO_2$ | 77.98 | 71.04 | 78.36 | 72.73 | 73.41 | 74.70 | 2.94 |
| $TiO_2$ | 0.15 | 0.12 | 0.18 | 0.16 | 0.20 | 0.16 | 0.03 |
| $Al_2O_3$ | 10.66 | 14.45 | 10.71 | 13.72 | 12.64 | 12.44 | 1.54 |
| FeO | 1.07 | 1.14 | 0.80 | 0.88 | 0.69 | 0.92 | 0.17 |
| MgO | 0.56 | 0.36 | 0.10 | 0.11 | 0.10 | 0.25 | 0.19 |
| CaO | 0.79 | 1.44 | 0.27 | 0.67 | 1.26 | 0.89 | 0.42 |
| $Na_2O$ | 2.12 | 3.24 | 2.32 | 2.43 | 2.43 | 2.51 | 0.38 |
| $K_2O$ | 2.40 | 3.52 | 4.23 | 6.97 | 4.88 | 4.40 | 1.53 |
| Total | 95.77 | 95.34 | 97.01 | 97.71 | 95.62 | 96.27 | |

*Total Fe as FeO.

*Values in wt%.

*n-number of analyses per sample.

Table 1. Continued.

| Sample | Brown Glass | | | Mean (b) | Std. Dev. | Mixed Glass | | Mean (T) | Std. Dev. |
|---|---|---|---|---|---|---|---|---|---|
| | WTB-2-2U n=6 | WTB-2A-2F n=4 | WTB-2-2G n=2 | | | WTB-2-2M n=3 | WTB-2-2F n=6 | | |
| $SiO_2$ | 79.95 | 71.83 | 75.93 | 75.90 | 3.32 | 72.07 | 89.88 | 74.81 | 3.11 |
| $TiO_2$ | 0.08 | 0.13 | 0.23 | 0.15 | 0.06 | 0.14 | 0.02 | 0.15 | 0.04 |
| $Al_2O_3$ | 9.30 | 13.38 | 11.13 | 11.27 | 1.67 | 13.71 | 4.11 | 12.19 | 1.68 |
| FeO | 0.84 | 1.51 | 0.50 | 0.95 | 0.42 | 0.59 | 0.13 | 0.89 | 0.29 |
| MgO | 0.57 | 1.40 | 0.13 | 0.70 | 0.53 | 0.04 | 0.06 | 0.37 | 0.41 |
| CaO | 0.43 | 3.06 | 0.16 | 1.22 | 1.31 | 0.10 | 0.16 | 0.91 | 0.88 |
| $Na_2O$ | 2.62 | 3.15 | 1.39 | 2.39 | 0.74 | 1.22 | 1.01 | 2.32 | 0.65 |
| $K_2O$ | 3.14 | 2.12 | 7.26 | 4.17 | 2.22 | 10.58 | 1.93 | 5.01 | 2.61 |
| Total | 96.96 | 96.62 | 96.75 | 96.75 | | 98.47 | 97.33 | 96.65 | |

*Total Fe as FeO.

*Values in wt%.

*n-number of analyses per sample.

*Mean (b)-mean of samples with brown glass.

*Mean (T)-"total" mean of all samples in Table 1.

Table 1a. Electron microprobe analyses of glasses from Lake Wanapitei by various authors.

| | Current work | | Dence et al., 1972 | Dence et al., 1974 | | Winzer, 1976 | |
|---|---|---|---|---|---|---|---|
| | Clear glass | Brown glass | Clear glass with lechatelierite | Clear glass | Brown glass | Clear glass | Brown glass |
| $SiO_2$ | 74.70 | 75.90 | 75.10 | 65.94 | 75.95 | 76.77 | 76.64 |
| $Al_2O_3$ | 12.44 | 11.27 | 9.30 | 20.15 | 13.85 | 10.80 | 11.11 |
| FeO | 0.92 | 0.95 | 2.30 | 0.17 | 2.07 | 1.83 | 1.64 |
| MgO | 0.25 | 0.70 | 1.20 | 0.09 | 1.42 | 1.04 | 0.98 |
| CaO | 0.89 | 1.22 | 1.10 | 0.23 | 0.12 | 0.95 | 1.12 |
| $Na_2O$ | 2.51 | 2.39 | 2.50 | 4.15 | 1.41 | 2.29 | 2.31 |
| $K_2O$ | 4.40 | 4.17 | 3.20 | 9.15 | 5.02 | 3.73 | 3.57 |

*All data in wt%.

*Current work data from Table 1.

*Dence et al., 1974 data are mean of four.

*Winzer, 1976 data are mean of two.

Table 1b. Normative calculations of glasses from Lake Wanapitei.

| | Current work | | Dence et al., 1972 |
|---|---|---|---|
| | Clear glass | Brown glass | Clear glass with lechatelierite |
| Quartz | 41.82 | 43.03 | 44.58 |
| Corundum | 2.00 | 0.62 | - |
| Orthoclase | 27.08 | 25.53 | 19.96 |
| Albite | 22.10 | 20.93 | 22.31 |
| Anorthite | 4.51 | 6.27 | 4.95 |
| Diopside | - | - | 0.54 |
| Hedenbergite | - | - | 0.66 |
| Enstatite | 0.65 | 1.81 | 2.90 |
| Ferrosilite | 1.76 | 1.81 | 4.10 |

Table 1b. Continued.

| | Dence et al., 1974 | | Winzer, 1976 | |
|---|---|---|---|---|
| | Clear glass | Brown glass | Clear glass | Brown glass |
| Quartz | 5.98 | 44.48 | 45.22 | 45.49 |
| Corundum | 3.00 | 5.88 | 1.30 | 1.44 |
| Orthoclase | 54.19 | 29.74 | 22.65 | 21.69 |
| Albite | 35.15 | 11.95 | 19.89 | 20.07 |
| Anorthite | 1.14 | 0.60 | 4.84 | 5.71 |
| Diopside | - | - | - | - |
| Hedenbergite | - | - | - | - |
| Enstatite | 0.22 | 2.66 | 3.54 | 2.51 |
| Ferrosilite | 0.31 | 3.45 | 3.81 | 3.09 |

Table 1c. Electron microprobe analyses of clear glass in sample WTB-2-2X.

| Target | 001 | 002 | Mean | 001 | 002 | 003 | 004 | 005 | 006 | Mean | Std. Dev. |
|---|---|---|---|---|---|---|---|---|---|---|---|
| $SiO_2$ | 98.01 | 98.34 | 98.18 | 69.16 | 70.79 | 71.63 | 73.44 | 71.31 | 71.15 | 71.24 | 1.26 |
| $TiO_2$ | 0.00 | 0.00 | 0.00 | 0.19 | 0.20 | 0.18 | 0.21 | 0.20 | 0.20 | 0.20 | 0.01 |
| $Al_2O_3$ | 0.12 | 0.02 | 0.07 | 14.05 | 13.84 | 14.48 | 14.60 | 13.56 | 14.64 | 14.20 | 0.41 |
| FeO | 0.03 | 0.02 | 0.03 | 2.36 | 1.79 | 0.98 | 0.79 | 1.93 | 0.66 | 1.42 | 0.64 |
| MgO | 0.01 | 0.03 | 0.02 | 1.66 | 0.91 | 0.28 | 0.15 | 1.38 | 0.09 | 0.75 | 0.61 |
| CaO | 0.01 | 0.01 | 0.01 | 1.08 | 1.02 | 1.10 | 1.08 | 0.97 | 1.06 | 1.05 | 0.04 |
| $Na_2O$ | 0.05 | 0.01 | 0.03 | 2.85 | 3.27 | 3.19 | 1.52 | 3.00 | 3.10 | 2.82 | 0.60 |
| $K_2O$ | 0.03 | 0.00 | 0.02 | 3.09 | 3.22 | 3.23 | 2.55 | 3.04 | 4.04 | 3.20 | 0.44 |
| Total | 98.26 | 98.43 | 98.33 | 94.44 | 95.04 | 95.07 | 94.34 | 95.39 | 94.94 | 94.86 | |

*All data in wt%.

Table 1d. Electron microprobe analyses of clear glass in sample WTB-2-2C.

| Target | 001 | 002 | 003 | 004 | 005 | 006 | 007 | Mean | Std. Dev. |
|---|---|---|---|---|---|---|---|---|---|
| $SiO_2$ | 100.0 | 74.29 | 73.91 | 75.67 | 74.18 | 73.95 | 72.67 | 74.11 | 0.88 |
| $TiO_2$ | 0.01 | 0.18 | 0.18 | 0.20 | 0.15 | 0.18 | 0.30 | 0.20 | 0.05 |
| $Al_2O_3$ | 0.05 | 12.28 | 12.92 | 12.01 | 13.01 | 12.66 | 13.52 | 12.73 | .49 |
| FeO | 0.00 | 0.60 | 0.80 | 0.57 | 0.69 | 0.60 | 0.69 | 0.66 | 0.08 |
| MgO | 0.00 | 0.05 | 0.08 | 0.06 | 0.11 | 0.07 | 0.09 | 0.08 | 0.02 |
| CaO | 0.02 | 0.27 | 0.35 | 0.08 | 0.13 | 0.31 | 0.40 | 0.26 | 0.12 |
| $Na_2O$ | 0.18 | 2.52 | 3.02 | 2.21 | 2.50 | 2.30 | 3.31 | 2.64 | 0.39 |
| $K_2O$ | 0.08 | 5.51 | 4.83 | 6.06 | 6.26 | 5.86 | 4.99 | 5.86 | 0.53 |
| Total | 100.34 | 95.70 | 96.09 | 96.86 | 97.03 | 95.93 | 95.97 | 96.26 | |

*All data in wt%.

*Column 001 is clear silica glass excluded from statistical calculations.

this trend. Unlike the microprobe, they show the bulk composition of the rock and thus, are unable to pick up the compositional differences within the clear glass.

Microprobe analyses show that the colouring of the Wanapitei glasses is not dependent upon major element composition. It is possible that the colouring is due to a dispersed phase or minor elements (Winzer et al., 1976). The variation in mafic content (Table 1b) may result from local inhomogeneities in glasses associated with melting of Mg-Fe rich phases, possibly signalling a contribution from diabase (Winzer et al., 1976).

The whole rock analyses (this work) are presented in Table 2. The major elements are given in wt%, the trace elements in ppm. Calibration range, estimate of error, and determination limits for major elements are included in Table 2a. The estimate of error in analyses of trace elements is shown in Table 2b. The analyses indicate a relatively consistent composition for the vesicular glassy melts expressed by low values of standard deviation (Table 2), except for sample WTB-2-2F, which is characterized by higher content of $SiO_2$, possibly resulting from a more quartzitic character of the protolith. Suevite breccia (sample WTB-3S-90, Table 2) displays a much lower content of $SiO_2$ (56.10 wt%) and higher concentration of MgO and CaO (5.74 wt% and 5.25 wt% respectively). The trends observed in these analyses compare to the microprobe results. Table 3 presents the siderophile data (except for Cr) on vesicular glassy melts from

Table 2. Chemical analyses of Lake Wanapitei impact melt rocks.

| Sample | WTB-2-2X | WTB-2T-90 | WTB-2-2F | WTB-2-2C | WTB-2A-2E | WTB-2-2KA | WTB-2A-2F | WTB-2-2G | WTB-2-2M | Mean | Std. Dev. |
|---|---|---|---|---|---|---|---|---|---|---|---|
| $SiO_2$ | 73.40 | 72.90 | 86.70 | 74.90 | 75.00 | 76.90 | 76.40 | 75.20 | 76.50 | 75.16 | 1.28 |
| $TiO_2$ | 0.19 | 0.19 | 0.06 | 0.19 | 0.19 | 0.21 | 0.20 | 0.20 | 0.20 | 0.20 | 0.01 |
| $Al_2O_3$ | 12.60 | 11.90 | 6.30 | 12.70 | 12.10 | 10.70 | 11.10 | 10.90 | 10.60 | 11.52 | 0.77 |
| $Cr_2O_3$ | 0.01 | 0.00 | 0.00 | 0.01 | 0.00 | 0.01 | 0.01 | 0.01 | 0.01 | 0.01 | 0.00 |
| $Fe_2O_3$ | 0.60 | 0.50 | 0.50 | 0.70 | 0.50 | 0.60 | 0.90 | 0.70 | 0.30 | 0.59 | 0.16 |
| FeO | 1.30 | 1.30 | 0.30 | 1.10 | 1.30 | 1.60 | 1.70 | 1.60 | 1.90 | 1.39 | 0.47 |
| MnO | 0.02 | 0.02 | 0.02 | 0.03 | 0.02 | 0.03 | 0.03 | 0.03 | 0.03 | 0.03 | 0.00 |
| MgO | 1.03 | 0.96 | 0.48 | 0.66 | 1.00 | 1.79 | 1.78 | 2.03 | 1.74 | 1.41 | 0.42 |
| CaO | 0.78 | 0.83 | 0.05 | 0.87 | 0.88 | 1.29 | 1.55 | 1.14 | 1.27 | 1.07 | 0.25 |
| $Na_2O$ | 3.00 | 2.80 | 0.40 | 3.10 | 2.80 | 1.70 | 2.20 | 1.50 | 1.70 | 2.31 | 0.59 |
| $K_2O$ | 2.59 | 2.92 | 0.90 | 2.62 | 3.09 | 2.64 | 2.09 | 1.99 | 2.70 | 2.47 | 0.45 |
| $H_2O$ | 3.90 | 3.40 | 3.70 | 2.50 | 2.90 | 2.50 | 1.70 | 3.50 | 2.40 | 2.94 | 0.69 |
| $CO_2$ | 0.30 | 2.20 | 0.80 | 0.40 | 0.10 | 0.20 | 0.10 | 0.40 | 0.40 | 0.54 | 0.62 |
| $P_2O_5$ | 0.06 | 0.06 | 0.04 | 0.06 | 0.06 | 0.05 | 0.05 | 0.05 | 0.05 | 0.05 | 0.01 |
| S | 0.03 | 0.01 | 0.03 | 0.04 | 0.01 | 0.03 | 0.02 | 0.03 | 0.01 | 0.02 | 0.01 |
| Total | 99.79 | 100.01 | 100.28 | 100.06 | 99.95 | 100.45 | 99.83 | 99.48 | 99.61 | 99.71 | |
| Trace elements | | | | | | | | | | | |
| Ba | 450 | 500 | 250 | 430 | 500 | 450 | 420 | 380 | 420 | 420 | 72 |
| Be | 1.6 | 1.6 | 0.7 | 1.6 | 1.5 | 1.4 | 1.3 | 1.4 | 1.4 | 1.4 | 0.3 |
| Co | 10 | 9 | 4 | 10 | 9 | 15 | 15 | 17 | 14 | 11 | 3.9 |
| Cr | 42 | 37 | 19 | 42 | 43 | 60 | 65 | 67 | 61 | 48 | 15 |
| Cu | 10 | 11 | 87 | 70 | 14 | 46 | 56 | 83 | 64 | 49 | 29 |
| La | 13 | 13 | 10 | 23 | 13 | 14 | 12 | 11 | 12 | 13 | 3.6 |
| Nb | 9 | 8 | 10 | 7 | 10 | 11 | 11 | 9 | 10 | 9 | 1.3 |
| Ni | 56 | 47 | 26 | 59 | 48 | 140 | 140 | 140 | 130 | 87 | 48 |
| Rb | 79 | 66 | 30 | 75 | 81 | 73 | 50 | 54 | 78 | 67 | 17.5 |
| Sr | 100 | 110 | 31 | 120 | 110 | 100 | 110 | 86 | 97 | 96 | 25 |
| V | 20 | 20 | 5 | 21 | 22 | 22 | 43 | 32 | 31 | 25 | 10 |
| Y | 6 | 6 | 3 | 5 | 6 | 6 | 6 | 5 | 6 | 5 | 1 |
| Yb | 0.5 | 0.5 | 0.3 | 0.5 | 0.5 | 0.5 | 0.5 | 0.4 | 0.6 | 0.5 | 0.1 |
| Zn | 0 | 26 | 66 | 110 | 15 | 49 | 240 | 220 | 33 | 84 | 84 |
| Zr | 84 | 81 | 40 | 77 | 83 | 69 | 66 | 73 | 68 | 71 | 13 |
| Ce | 30 | 29 | 23 | 55 | 28 | 26 | 29 | 26 | 28 | 36 | 18 |
| Dy | 2 | 1.4 | 0.7 | 1.3 | 1.2 | 1.2 | 1.4 | 1.1 | 1.3 | 1.3 | 0.3 |
| Eu | 0.6 | 0.5 | 0.2 | 0.7 | 0.5 | 0.4 | 0.5 | 0.4 | 0.5 | 0.5 | 0.1 |

Table 2. Continued. Chemical analyses of Lake Wanapitei impact melt rocks

| Sample | WTB 2 2X | WTB-2T-90 | WTB-2-2F | WTB-2-2C | WTB-2A-2E | WTB 2 2WA | WTB-2A 2F | WTB-2-2G | WTB-2-2M | Mean | Std. Dev. |
|---|---|---|---|---|---|---|---|---|---|---|---|
| Gd | 3 | 1.6 | 0.8 | 1 9 | 1.4 | 1.4 | 1 5 | 1.2 | 1.5 | 1 6 | 0 6 |
| Nd | 33 | 18 | 9.5 | 26 | 19 | 1 7 | 16 | 15 | 17 | 17 | 8 |
| Sm | 4.6 | 2.3 | 1.1 | 3 2 | 2 | 2 | 21 | 1 5 | 1.6 | 4 4 | 6 |

*Major elements in wt%.

*Trace elements in ppm.

*All samples are vesicular glassy melt rocks.

Table 2. Continued, impact breccias.

| Sample | WTB-3S-90 | WTB-2-2U | Mean of all samples | Std. Dev. |
|---|---|---|---|---|
| $SiO_2$ | 56.10 | 75.20 | 74.47 | 6.78 |
| $TiO_2$ | 0.45 | 0.20 | 0.21 | 0.03 |
| $Al_2O_3$ | 14.00 | 11.10 | 11.27 | 0.62 |
| $Cr_2O_3$ | 0.02 | 0.01 | 0.01 | 0.00 |
| $Fe_2O_3$ | 3.80 | 1.50 | 0.96 | 0.31 |
| FeO | 2.90 | 0.80 | 1.47 | 0.21 |
| MnO | 0.12 | 0.03 | 0.03 | 0.01 |
| MgO | 5.74 | 1.48 | 1.72 | 0.45 |
| CaO | 5.25 | 1.00 | 1.35 | 0.43 |
| $Na_2O$ | 1.60 | 2.00 | 2.07 | 0.26 |
| $K_2O$ | 1.62 | 1.62 | 2.25 | 0.21 |
| $H_2O$ | 7.80 | 4.40 | 3.52 | 0.51 |
| $CO_2$ | 0.60 | 0.20 | 0.52 | 0.19 |
| $P_2O_5$ | 0.05 | 0.05 | 0.05 | 0.00 |
| S | 0.02 | 0.00 | 0.02 | 0.00 |
| Total | 100.07 | 99.59 | 99.94 | |
| Trace elements | | | | |
| Ba | 690 | 340 | 437 | 106 |
| Be | 1.0 | 1.6 | 1.4 | 0.3 |
| Co | 36 | 13 | 14 | 8 |
| Cr | 120 | 41 | 54 | 25 |
| Cu | 110 | 38 | 54 | 32 |
| La | 22 | 11 | 14 | 4 |
| Nb | 0 | 8 | 8 | 3 |
| Ni | 150 | 78 | 92 | 45 |

Table 2. Continued. Impact breccias.

| Sample | WTB-3S-90 | WTB-2-2U | Mean of all samples | Std. Dev. |
|---|---|---|---|---|
| Rb | 53 | 49 | 64 | 17 |
| Sr | 500 | 95 | 133 | 118 |
| V | 110 | 33 | 33 | 26 |
| Y | 8 | 4 | 6 | 1 |
| Yb | 0.5 | 0.4 | 0.6 | 0.1 |
| Zn | 42 | 0 | 73 | 80 |
| Zr | 48 | 74 | 70 | 13 |
| Ce | 47 | 24 | 36 | 17 |
| Dy | 1.7 | 1 | 1.3 | 0.3 |
| Eu | 0.6 | 0.4 | 0.5 | 0.1 |
| Gd | 1.9 | 1.4 | 1.6 | 0.5 |
| Nd | 35 | 1.7 | 20 | 7.5 |
| Sm | 2.2 | 2 | 2.2 | 0.9 |

*Major elements in wt%.

*Trace elements in ppm.

*WTB-3S-90 is suevite breccia.

*WTB-2-2U is polymict breccia.

Table 2a. Estimate of precision of analyses of major elements (from Table 2).

| $SiO_2$ | $TiO_2$ | $Al_2O_3$ | $Cr_2O_3$ | $Fe_2O_3$ | FeO | MnO | MgO | CaO | $Na_2O$ | $K_2O$ | $H_2O$ | $CO_2$ | $P_2O_5$ | S |
|---|---|---|---|---|---|---|---|---|---|---|---|---|---|---|
| 0.40 | 0.02 | 0.40 | 0.02 | 0.20 | 0.20 | 0.01 | 0.10 | 0.10 | 0.50 | 0.05 | 0.10 | 0.05 | 0.02 | 0.04 |

*Precision in +/- wt% of concentration.

Table 2b. Estimate of precision of analyses of trace elements from Table 2).

| Ba | Be | Co | Cr | Cu | La | Nb | Ni | Pb | Sr | Sm | Y | Yb | Zn | Zr | Ce | Dy | Eu | Gd | Nd | V |
|---|---|---|---|---|---|---|---|---|---|---|---|---|---|---|---|---|---|---|---|---|
| 20 | 0.5 | 5 | 10 | 10 | 10 | 30 | 10 | 20 | 20 | 0.3 | 5 | 0.5 | 5 | 20 | 0.5 | 0.2 | 0.1 | 0.2 | 0.5 | 5 |

*Precision in +/- ppm.

*Ba to Zr analyzed by ICP-TR1.

*Ce to V analyzed by ICP-RE1.

Table 3. "Meteoritic" elements in Wanapitei impact melt rocks.

| Sample | MSWX-137-70 | MSWX-154-70 | MSWX-200-70 | Mean |
|---|---|---|---|---|
| Co (ppm) | 10.4 | 10.6 | 13.2 | 11.4 |
| Cr (ppm) | 45 | 58 | 65 | 56 |
| Ni (ppm) | 103 | 85.7 | 136 | 108 |
| Os (ppb) | 1.9 | 1.2 | 3.2 | 2.1 |
| Ir (ppb) | 2.07 | 2.05 | 2.86 | 2.33 |
| Pd (ppb) | 2.37 | 3.30 | 4.60 | 3.42 |
| Au (ppb) | 3.08 | 2.38 | 8.32 | 4.59 |
| Ge (ppb) | 1018 | 752 | 992 | 921 |
| Se (ppb) | 5.6 | 9.3 | 19.2 | 11.4 |
| Re (ppb) | 0.074 | 0.101 | 0.143 | 0.106 |

*All data from Wolf et al., 1980 and N.Evans, personal communication.

*Pd, Au, are mean of 2: 1 from Wolf et al. (1980), and 1 from N.Evans (personal communication).

*Co, Cr, Ni, Os, Ge, Se, Re from Wolf et al. (1980).

Table 4. Chemical analyses of rocks of the Gowganda Formation.

| Sample | 001 | 002 | 003 | 004 | 005 | 006 | 007 |
|---|---|---|---|---|---|---|---|
| $SiO_2$ | 51.20 | 60.40 | 59.10 | 57.76 | 65.14 | 73.20 | 71.30 |
| $TiO_2$ | 0.95 | 0.73 | 0.82 | 0.75 | 0.60 | 0.19 | 0.20 |
| $Al_2O_3$ | 21.90 | 19.40 | 16.50 | 17.82 | 14.80 | 11.40 | 13.70 |
| $Cr_2O_3$ | 0.00 | 0.00 | 0.00 | 0.00 | 0.00 | 0.00 | 0.00 |
| $Fe_2O_3$ | 2.40 | 3.42 | 4.69 | 2.87 | 3.68 | 0.25 | 0.68 |
| FeO | 2.76 | 4.94 | 5.31 | 4.96 | 3.69 | 1.00 | 2.00 |
| MnO | 0.07 | 0.11 | 0.13 | 0.00 | 0.00 | 0.05 | 0.04 |
| MgO | 5.92 | 2.70 | 3.21 | 4.16 | 3.56 | 0.64 | 1.22 |
| CaO | 0.40 | 0.65 | 1.55 | 1.22 | 1.50 | 3.09 | 0.63 |
| $Na_2O$ | 5.14 | 2.33 | 2.91 | 3.15 | 4.39 | 5.23 | 4.07 |
| $K_2O$ | 2.63 | 3.01 | 2.98 | 3.36 | 1.72 | 1.55 | 3.97 |
| $H_2O$ | 4.16 | 3.65 | 2.78 | 3.19 | 2.73 | 0.55 | 1.06 |
| $CO_2$ | 0.06 | 0.20 | 0.25 | 0.00 | 0.00 | 2.51 | 0.28 |
| $P_2O_5$ | 0.14 | 0.14 | 0.15 | 0.23 | 0.16 | 0.04 | 0.05 |
| S | 0.01 | 0.01 | 0.04 | 0.00 | 0.00 | 0.07 | 0.05 |
| Total | 97.74 | 101.69 | 100.42 | 99.47 | 101.97 | 99.77 | 99.25 |
| Trace elements | | | | | | | |
| Be | - | - | - | - | - | 0 | 1 |
| Co | - | - | - | - | - | 5 | 7 |
| Cu | - | - | - | - | - | 44 | 200 |
| Ni | - | - | - | - | - | 10 | 24 |
| Sc | - | - | - | - | - | 6 | 5 |
| Sr | - | - | - | - | - | 106 | 131 |
| V | - | - | - | - | - | 26 | 49 |
| Y | - | - | - | - | - | 11 | 5 |
| Zn | - | - | - | - | - | 10 | 26 |

*Major elements in wt%.

*Trace elements in ppm.

*001 to 003-Laminated siltstone-argillite; Card (1978).

*004-Laminated argillite, average of 9; Card (1978).

*005-Paraconglomerate matrix; Young (1969).

*006 and 007-Sandstone; Junnila (1990).

Table 4. Continued.

| Sample | 008 | 009 | 010 | 011 | 012 | 013 | Mean | Std. Dev. |
|---|---|---|---|---|---|---|---|---|
| $SiO_2$ | 80.50 | 60.80 | 62.60 | 65.50 | 61.50 | 81.30 | 65.41 | 8.53 |
| $TiO_2$ | 0.15 | 0.47 | 0.32 | 0.42 | 0.50 | 0.09 | 0.48 | 0.27 |
| $Al_2O_3$ | 11.00 | 16.40 | 17.20 | 15.50 | 16.90 | 10.40 | 15.61 | 3.22 |
| $Cr_2O_3$ | 0.00 | 0.00 | 0.00 | 0.00 | 0.00 | 0.00 | 0.00 | 0.00 |
| $Fe_2O_3$ | 0.00 | 1.95 | 1.24 | 1.02 | 1.52 | 0.17 | 1.84 | 1.43 |
| FeO | 0.47 | 4.86 | 3.53 | 3.73 | 4.19 | 0.33 | 3.21 | 1.69 |
| MnO | 0.01 | 0.07 | 0.07 | 0.07 | 0.07 | 0.01 | 0.05 | 0.04 |
| MgO | 0.41 | 2.64 | 2.26 | 2.24 | 2.94 | 0.21 | 2.47 | 1.55 |
| CaO | 0.24 | 1.09 | 1.07 | 1.25 | 1.22 | 0.32 | 1.09 | 0.71 |
| $Na_2O$ | 5.85 | 3.75 | 5.27 | 4.36 | 3.65 | 5.57 | 4.28 | 1.05 |
| $K_2O$ | 0.08 | 3.34 | 3.45 | 2.90 | 3.41 | 0.08 | 2.50 | 1.22 |
| $H_2O$ | 0.42 | 2.79 | 1.33 | 1.70 | 2.39 | 0.28 | 2.08 | 1.23 |
| $CO_2$ | 0.13 | 0.12 | 0.08 | 0.09 | 0.08 | 0.22 | 0.31 | 0.64 |
| $P_2O_5$ | 0.03 | 0.12 | 0.13 | 0.14 | 0.14 | 0.02 | 0.11 | 0.06 |
| S | 0.02 | 0.04 | 0.05 | 0.08 | 0.06 | 0.04 | 0.04 | 0.03 |
| Total | 99.31 | 98.32 | 98.60 | 99.00 | 98.58 | 99.04 | 99.47 | |
| Trace elements | | | | | | | | |
| Be | 0 | 2 | 2 | 2 | 2 | 0 | 2 | 0.4 |
| Co | 0 | 19 | 14 | 16 | 16 | 0 | 13 | 5 |
| Cu | 5 | 11 | 10 | 49 | 40 | 74 | 54 | 59 |
| Ni | 0 | 61 | 46 | 50 | 55 | 0 | 41 | 18 |
| Sc | 2 | 8 | 7 | 9 | 8 | 2 | 6 | 3 |
| Sr | 35 | 161 | 712 | 221 | 199 | 31 | 200 | 204 |
| Y | 12 | 105 | 72 | 84 | 94 | 13 | 57 | 35 |
| V | 7 | 8 | 6 | 8 | 8 | 0 | 8 | 2 |
| Zn | 7 | 62 | 66 | 69 | 65 | 5 | 39 | 27 |

*Major elements in wt%.

*Trace elements in ppm.

*008 to 013-Sandstone; Junnila (1990).

Table 5. Chemical analyses of rocks of the Mississagi Formation.

| Sample | 001 | 002 | 003 | 004 | 005 | Mean | Std. Dev. |
|---|---|---|---|---|---|---|---|
| $SiO_2$ | 88.50 | 86.13 | 86.01 | 83.91 | 89.73 | 86.86 | 2.04 |
| $TiO_2$ | 0.05 | 0.09 | 0.15 | 0.16 | 0.05 | 0.10 | 0.05 |
| $Al_2O_3$ | 6.11 | 7.68 | 7.87 | 9.71 | 3.19 | 6.91 | 2.18 |
| $Cr_2O_3$ | 0.00 | 0.00 | 0.00 | 0.00 | 0.00 | 0.00 | 0.00 |
| $Fe_2O_3$ | 0.31 | 0.00 | 0.11 | 0.69 | 0.60 | 0.34 | 0.27 |
| FeO | 0.22 | 0.58 | 0.40 | 0.77 | 0.70 | 0.53 | 0.20 |
| MnO | 0.01 | 0.00 | 0.00 | 0.00 | 0.00 | 0.00 | 0.00 |
| MgO | 0.13 | 0.18 | 0.54 | 0.78 | 0.54 | 0.43 | 0.24 |
| CaO | 0.10 | 0.23 | 0.05 | 0.06 | 0.45 | 0.18 | 0.15 |
| $Na_2O$ | 0.38 | 3.74 | 4.51 | 1.87 | 1.89 | 2.48 | 1.47 |
| $K_2O$ | 3.22 | 1.42 | 0.30 | 1.24 | 2.43 | 1.72 | 1.01 |
| $H_2O$ | 0.33 | 0.00 | 0.00 | 0.58 | 0.36 | 0.25 | 0.22 |
| $CO_2$ | 0.29 | 0.00 | 0.00 | 0.32 | 0.92 | 0.31 | 0.34 |
| $P_2O_5$ | 0.01 | 0.02 | 0.02 | 0.05 | 0.00 | 0.02 | 0.02 |
| S | 0.05 | 0.00 | 0.00 | 0.00 | 0.00 | 0.01 | 0.02 |
| Total | 99.71 | 100.05 | 99.96 | 100.14 | 100.86 | 100.14 | |
| Trace elements | | | | | | | |
| Ba | 400 | 200 | 0 | - | - | 200 | 163 |
| Co | 6 | 6 | 3 | - | - | 5 | 1 |
| Cr | 200 | 100 | 250 | - | - | 183 | 62 |
| Cu | 10 | 10 | 4 | - | - | 8 | 3 |
| Ni | 30 | 10 | 10 | - | - | 17 | 9 |
| Rb | 0 | 30 | 30 | - | - | 20 | 14 |
| Sr | 30 | 80 | 10 | - | - | 40 | 29 |
| V | 0 | 15 | 20 | - | - | 12 | 8 |
| Y | 20 | 0 | 0 | - | - | 7 | 9 |
| Zn | 6 | 8 | 10 | - | - | 8 | 2 |
| Zr | 30 | 20 | 30 | - | - | 27 | 5 |

*Major elements in wt%.

*Trace elements in ppm.

*001 to 003-Mississagi subarkose; Card (1978).

*004 and 005-Mississagi quartzite; 004-Speers (1957); 005-Thomson (1961).

Table 6. Chemical analyses of rocks of the Bruce Formation.

| Sample | 001 | 002 | Mean |
|---|---|---|---|
| $SiO_2$ | 73.50 | 70.55 | 72.03 |
| $TiO_2$ | 0.46 | 0.56 | 0.51 |
| $Al_2O_3$ | 11.92 | 12.10 | 12.01 |
| $Fe_2O_3$ | 1.39 | 0.88 | 1.13 |
| FeO | 1.88 | 3.64 | 2.76 |
| MgO | 2.18 | 2.02 | 2.10 |
| CaO | 0.20 | 1.64 | 0.92 |
| $Na_2O$ | 3.50 | 2.84 | 3.17 |
| $K_2O$ | 3.12 | 2.29 | 2.70 |
| $H_2O$ | 1.48 | 2.20 | 1.84 |
| $CO_2$ | 0.00 | 0.72 | 0.36 |
| $P_2O_5$ | 0.11 | 0.14 | 0.13 |
| Total | 99.74 | 99.58 | 99.65 |

*Data in wt%.

*001 and 002-Bruce paraconglomerate (Card, 1978).

Table 7. Chemical analyses of the Nipissing intrusive rocks.

| | Mean | Std. Dev. |
|---|---|---|
| $SiO_2$ | 57.84 | 8.71 |
| $TiO_2$ | 0.63 | 0.28 |
| $Al_2O_3$ | 13.88 | 2.35 |
| $Cr_2O_3$ | 0.02 | 0.06 |
| $Fe_2O_3$ | 2.44 | 1.89 |
| FeO | 5.79 | 2.78 |
| MnO | 0.13 | 0.07 |
| MgO | 5.44 | 3.28 |
| CaO | 8.21 | 5.21 |
| $Na_2O$ | 2.88 | 1.95 |
| $K_2O$ | 0.97 | 0.73 |
| $H_2O$ | 1.16 | 0.57 |
| $CO_2$ | 0.28 | 0.18 |
| $P_2O_5$ | 0.08 | 0.07 |
| S | 0.04 | 0.03 |
| Total | 99.79 | |
| Trace elements | | |
| Ag | 0.9 | 0.4 |
| As | 9 | 17 |
| Ba | 62 | 71 |
| Be | 0.5 | 0.7 |
| Co | 25 | 16 |
| Cr | 222 | 302 |
| Cu | 73 | 53 |
| Ga | 20 | 8 |
| Li | 16 | 12 |
| Mn | 812 | 673 |
| Mo | 5 | 4 |
| Ni | 93 | 70 |
| Pb | 10 | 0 |

Table 7. Continued.

| | Mean | Std. Dev. |
|---|---|---|
| Sb | 1 | 3 |
| Sc | 49 | 19 |
| Sn | 4 | 2 |
| Sr | 118 | 61 |
| Ti | 3462 | 2098 |
| V | 155 | 88 |
| Y | 21 | 3 |
| Zn | 58 | 28 |
| Zr | 77 | 68 |

*Major elements in wt%.

*Trace elements in ppm.

*Mean calculated from 22 samples:
-2 qtz.-plag. porphyry; Dressler, 1982.
-2 granophyre; Dressler, 1982.
-18 diabase; Card, 1978.

*Trace element mean calculated from 13 samples of diabase; Card, 1978.

the collection of Geological Survey of Canada, analyzed by Wolf et al. (1980) and Noreen Evans (personal communication). The samples come from the same area south of the Lake Wanapitei. The chemical analyses of target rocks used in this work come from the literature cited in the Tables 4 to 7. Mean values and standard deviations were calculated and are listed in those tables. The data were selected according to availability; thus, in part, the means or standard deviations may not express the true range of composition of the whole suite of lithologies from the formations they represent. Although, some of the data come from outcrops, which are not adjacent to the lake, however, the idea behind selection of the samples was, that they come the same formations and are petrologically very similar to the Wanapitei outcrops. The Huronian Supergroup was deposited (southwesterly) over an area of several hundred square kilometres and is relatively uniform throughout (Card, 1978). The clastic material came from erosion of granitic terrane to the north, so called Cobalt area (Dressler, 1982). Thus the samples chosen for the study come from locations close to Lake Wanapitei when compared to the entire area covered by the Huronian Supergroup sedimentation. Based on these facts, it is very likely that no significant compositional changes occur within the formations over the area of interest (Lake Wanapitei up to locations of samples). Following is the description of samples of target rocks chosen for the study.

The Gowganda Formation (Table 4) is represented by siltstone-argillite from the outcrops adjacent to the McGregor Bay (Lat. 46°00'N, Long. 82°30'W), Sudbury-Manitoulin area (Map 2360 and charts in Card, 1978), and by sandstone from the Yarrow and Doon Townships in the Cobalt area (sample locations in Junnila, 1990). The Mississagi Formation (Table 5), is represented by subarkose from Township 156, and by partly albitized subarkose from the outcrops around Kusk Lake (Lat. 46°17', Long. 81°19'W) and Nemag Lake (Lat. 46°20', Long. 81°14'), Sudbury-Manitoulin area (Map 2360 and charts in Card, 1978). The formation is also represented by quartzite from the northern margin of Ramsey Lake, southeast of Sudbury (Speers, 1957), and quartzite from the east shore of Massey Bay, in the south half of lot 6, concession V, Lake Wanapitei (Thomson, 1961). The Bruce Formation (Table 6), is represented by two analyses of paraconglomerate matrix from the Sudbury-Espanola area (Lat. 46°15'N, Long. 81°45'W), southwest of Sudbury (Card et al., 1977). The Nipissing Intrusives (Table 7) are represented by: feldspathic pyroxenite and actinolite-amphibolite from Drury Township (Lat. 46°25'N, Long. 81°34'W); metagabbro, granophyric gabbro, two-pyroxene gabbro, and granophyre from McGregor Bay (the same area as for the Gowganda silltstone-argillite samples); pyroxene gabbro and hornblende-metagabbro from Shakespeare Township; and metagabbro from the Mongowin Township, all in the Sudbury-Manitoulin area (Map 2360 and charts in Card,

1978).

Figures 7 and 8 show the ternary cation plots with the compositional fields of the suspected target rocks and the Wanapitei impact melt rocks. The general overlap of the impact melt compositions with the target rocks is evident for sediments of the Mississagi (Hough Lake Group, Figure 1) and Gowganda Formations (Cobalt Group, Figure 1). No correlation exists for the Nipissing rocks. When the Wanapitei melt rocks and Nipissing Intrusives are removed from the triangle (Figure 8), it appears that approximately a 50/50 contribution of the Mississagi and Gowganda rocks is necessary to match the compositional range of the Wanapitei impact melt samples. The Mississagi supplies the high $SiO_2$ content, whereas the Gowganda contributes the high $Al_2O_3$ to the melt rocks.

Figure 7. Cation plot of crater and target rocks, Lake Wanapitei impact structure.

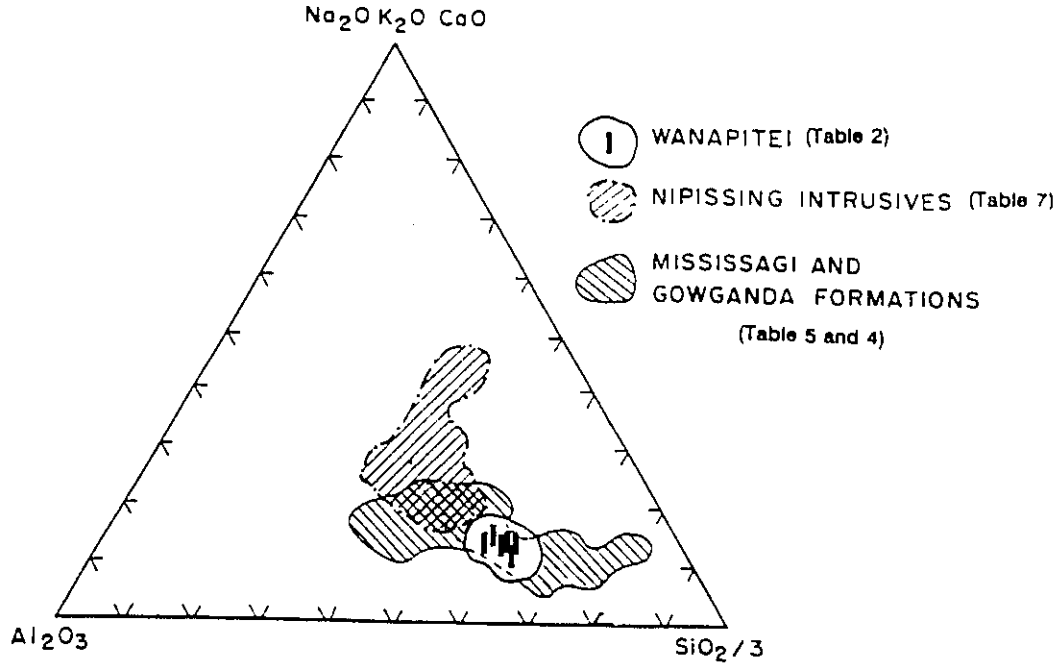


Figure 8. Cation plot of target rocks without Nipissing intrusives, Lake Wanapitei impact structure.

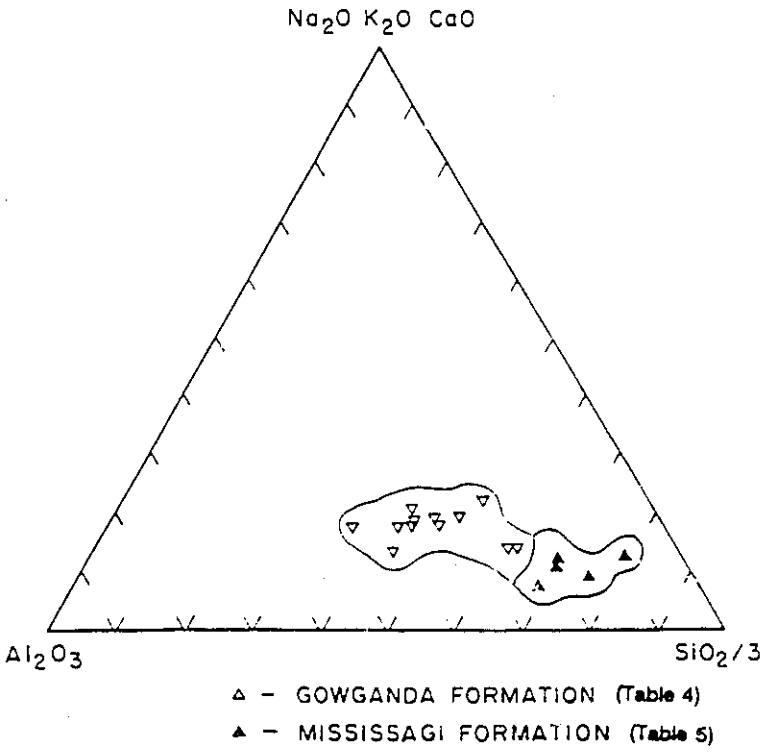

## Mixing Model

A least squares method for solving petrographic mixing equations, the mixing model, was applied using a modified computer program of Wright and Doherty (1970). Generally, one of the applications of the program can be "...evaluation of the possibility that a given magma type (represented by a single or an average rock analysis) could be described as a mixture of other magma types similarly represented.." (Wright and Doherty, 1970, p.1996). Theoretically, the program uses a mathematical technique of setting and solving a number of scalar equations:

$$X=\sum_{i=1}^{n} x_i y_i$$

where X is oxide in wt% after adjusting the whole analysis to 100% (the equation is formed for each of the oxides from the analysis of the rock), "x" is the weight percent of constituent X in mineral "i", and "y" is the weight percent of mineral "i" in the rock. The sum of $y_i$ is normalized to 100%.

For the present study, the "magma mixing" application of the program was used (Wright and Doherty, 1970). The data were input as mean chemical compositions (in wt%) of suspected target rocks and adjusted to 100% (X in the above equation). The mean of the Wanapitei impact melt rocks (Table 2) was used as the "supposed

magma" (melt observed in Table 8).

The computing role of the program was to define and solve ten linear equations (one for each oxide) and present a least squares type of approximation of which target rocks (Nipissing, Bruce, Mississagi, Gowganda; Table 8), and in what proportion, could contribute to form the "melt observed" (Wright and Doherty, 1970). All input data and the results are presented in Table 8 and Figure 9. The best match to the mean of the observed composition of the Wanapitei impact melt rocks was achieved by mixing the rocks of Mississagi and Gowganda Formations. The attempt to add sediments of the Bruce Formation and/or Nipissing Intrusives resulted in a complete rejection (Table 8). The solution of the mixing model, that is the calculated melt, represents a mix comprising 56.4% of the Mississagi Formation and 43.6% of the Gowganda Formation. The precision of the result is expressed by the reduced Chi-square value of the mix (reduced Chi-square=Chi-square/sum of oxides (10)-sum of target constituents (2)). It does not exceed the value of 1.00, which is considered a statistically good fit. The differences between the calculated and the observed mix fall within the values of standard deviations of the various oxides. The results stand in agreement with the previous works attempting to identify the target rocks without application of formal mixing models (Dence and Popelar, 1972; Dence et al., 1974; Winzer et al., 1976).

Table 8. Mixing model calculations.

| | Nipissing | Bruce | Mississagi | Gowganda | Melt observed | | Melt calculated | Difference Observ.-Calc. | Residuals Observ.-Calc. / Std. Dev. |
|---|---|---|---|---|---|---|---|---|---|
| | Mean | Mean | Mean | Mean | Mean | Std. Dev. | | | |
| $SiO_2$ | 57.84 | 72.03 | 86.86 | 65.41 | 74.47 | 6.78 | 77.51 | -3.04 | 0.45 |
| $TiO_2$ | 0.63 | 0.51 | 0.10 | 0.48 | 0.21 | 0.09 | 0.27 | -0.06 | 1.86 |
| $Al_2O_3$ | 13.88 | 12.01 | 6.91 | 15.61 | 11.27 | 1.86 | 10.70 | 0.57 | 0.31 |
| $Cr_2O_3$ | 0.02 | 0.00 | 0.00 | 0.00 | 0.01 | 0.01 | 0.00 | 0.01 | 1.00 |
| FeOT | 7.99 | 3.13 | 0.84 | 4.87 | 2.38 | 1.29 | 2.60 | -0.22 | 0.17 |
| MnO | 0.13 | - | - | 0.05 | 0.03 | 0.03 | 0.02 | 0.01 | 0.27 |
| MgO | 5.44 | 2.10 | 0.43 | 2.47 | 1.72 | 1.35 | 1.32 | 0.40 | 0.30 |
| CaO | 8.21 | 0.92 | 0.18 | 1.09 | 1.35 | 1.29 | 0.58 | 0.77 | 0.60 |
| $Na_2O$ | 2.88 | 3.17 | 2.48 | 4.28 | 2.07 | 0.78 | 3.27 | -1.20 | 1.53 |
| $K_2O$ | 0.97 | 2.70 | 1.72 | 2.50 | 2.25 | 0.84 | 2.06 | 0.19 | 0.30 |

*Wanapitei data from Table 2.

*Nipissing data from Table 7.

*Bruce data from Table 6.

*Mississagi data from Table 5.

*Gowganda data from Table 4.

*FeOT calculated from FeOT = Fe2O3 x 0.8998 + FeO

*Solution is a mix of 56.41% of Mississagi and 43.59% of Gowganda, 0% of Nipissing and 0% of Bruce.

*Chi-square = 7.7185

*Reduced Chi-square = 0.96481

Figure 9. Mixing model results; melt observed vs. melt calculated.

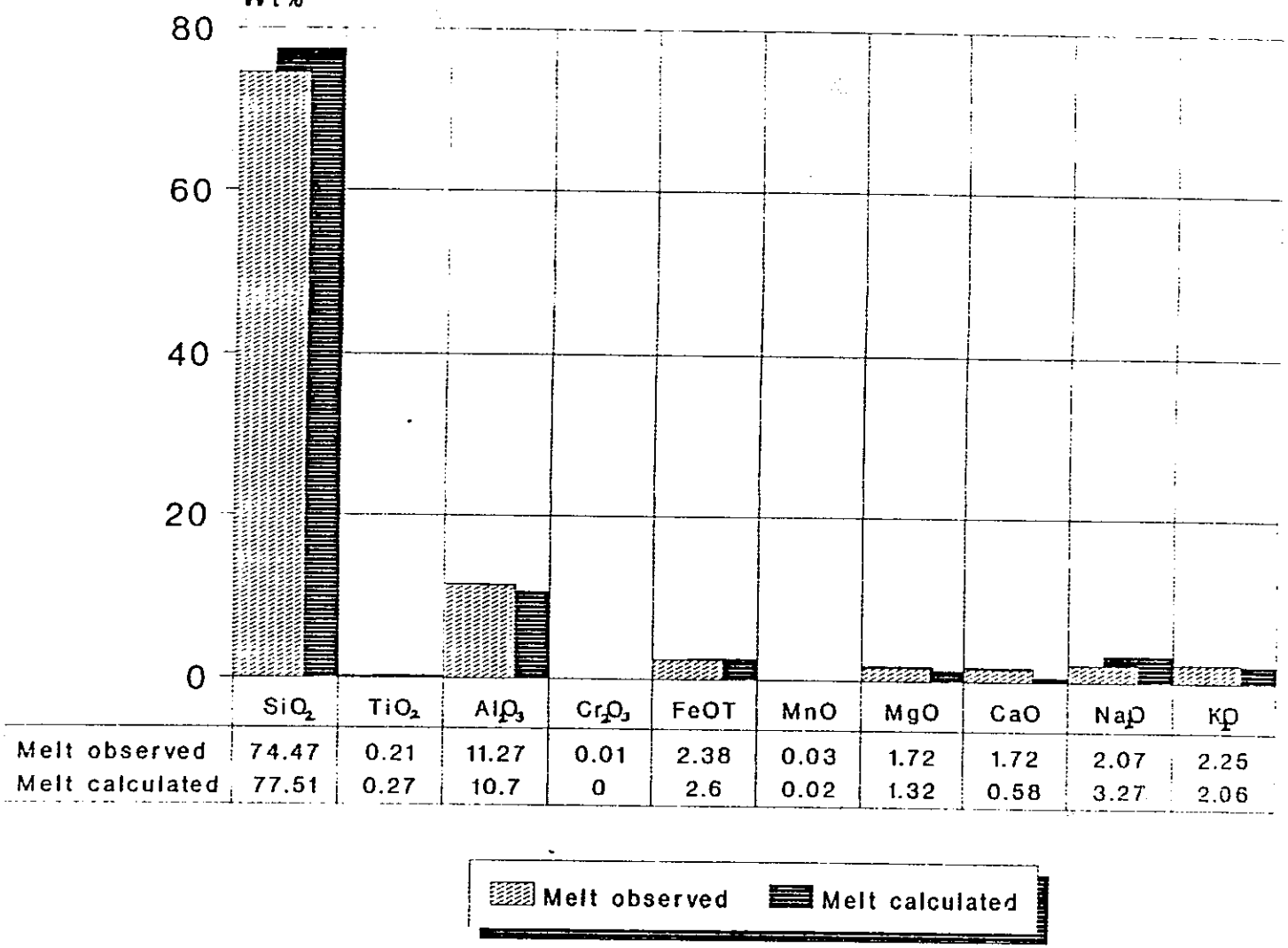


| | $SiO_2$ | $TiO_2$ | $Al_2O_3$ | $Cr_2O_3$ | FeOT | MnO | MgO | CaO | $Na_2O$ | $K_2O$ |
|---|---|---|---|---|---|---|---|---|---|---|
| Melt observed | 74.47 | 0.21 | 11.27 | 0.01 | 2.38 | 0.03 | 1.72 | 1.72 | 2.07 | 2.25 |
| Melt calculated | 77.51 | 0.27 | 10.7 | 0 | 2.6 | 0.02 | 1.32 | 0.58 | 3.27 | 2.06 |

The $Na_2O$, $TiO_2$, and $Cr_2O_3$ have the highest residual values (Table 8), which make them the poorest matching elements in the calculated mix. The volume of Nipissing dikes in the area of interest is not greater than 1 to 2%. Thus, it is reasonable that they do not form a component in the least squares mixing model. Considering the regional distribution of the Nipissing dikes and lack of compositional overlap from the ternary cation plot (Figure 7), it appears unlikely that Nipissing rocks could have taken a part in the formation of the impact melts. Despite many configurations of input data fed into the mixing program, the presence of Nipissing content offsets the results; yielding much higher residual values and a reduced Chi-square value well in excess of the desired precision limit. The trace element mixing model was not performed due to the insufficient data available for target rocks. The mixing model shows that based upon averaged chemical data, it is statistically reasonable that the Mississagi and Gowganda Formations played a major part in formation of Wanapitei impact melt rocks. The calculations are geologically significant by pointing at the most probable (from the perspective of geological setting of the rocks) choice for target lithologies among the varieties of country rocks.

Note: The results of the mixing model presented in this study have been obtained from mean values calculated for each of the target rocks. The author does not exclude such possibility, that a particular melt rock consists of fragments of all four

suspected target rocks (including those rejected by the statistical calculations). Also, the study could have been extended using either the individual rock analyses, instead of mean values, or mean values representing a much larger set of analyses of target- or shock metamorphosed rocks.

## Meteoritic Content

One of the potential features of a meteoritic impact site is the chemical trace that the projectile leaves in the impact lithologies, even after being melted and vaporized. This chemical trace enables the identification of the type of projectile and can serve as an indication that the meteoritic impact has occurred. The chemical composition of some meteorites differs from that of the Earth's crust, with respect to certain groups of elements. Due to differentiation processes during formation, the Earth's crust is generally depleted in elements such, as Ir, Ni, Os, Co, and Pd. On the contrary, the undifferentiated meteorites are considerably enriched in these elements with respect to the earth's crust. Moreover, the ratios of these elements in meteorites are relatively fixed and may survive through the impact and destruction of the meteoritic body.

The search for meteoritic content in impact melt rocks has been performed at several terrestrial impact craters; for example, at Meteor, Wabar, Aouelloul, and Mistastin craters (Morgan et al., 1975), Rochechouart structure (Janssens et al., 1977), Clearwater East and West, and Manicouagan craters (Palme et al., 1978) and other impact sites including the Gow Lake, Mistastin, Nicholson Lake, and Wanapitei Lake craters (Wolf et al., 1980). The meteoritic content in impact melt rocks is defined as the

"net meteoritic component" (Wolf et al., 1980, p.1017). The net component is obtained by subtraction of an indigenous component from the gross abundances of the elements under study. A previous investigation of the meteoritic content in shocked rocks from the Wanapitei structure has been carried out by Wolf et al., (1980). Using two samples of basement quartzite and three samples of inclusion-rich glassy melt from the glacial float, the researchers found an LL-chondrite to be the best approximation to the impacting body, but that C1 or C2 are not excluded.

The calculations of indigenous content (Table 9) utilize the proportion of target rocks derived by the mixing model. The Au, Ge, and Se have been left uncorrected due to the problematic depletion in these elements of the impact melt rocks versus the country rocks. This situation has been noted earlier by Wolf et al. (1980). Gold in the Lake Wanapitei area is locally concentrated in hydrothermal quartz veins associated with Nipissing intrusions, which cut through the Huronian sediments. The level of concentration is ≤11 ppm (data from Lake Wanapitei Nipissing Gabbro Intrusion; Dressler, 1982, p.102). The values reported by Wolf et al. (1980, p.1017) for the Lake Wanapitei impact melt rock (Table 3) show a much lower concentration (about 1000 times lower) and an irregular distribution (Wolf et al, 1980; N.Evans, personal communication). Thus, the mean values calculated for Au data have little meaning, with respect

to the element's distribution, making the indigenous correction impossible. The depletion of Ge and Se in the Wanapitei impact rocks versus target rocks (Table 9) has been ascribed to volatilization of the elements during the impact (Wolf et al., 1980).

Table 10 and Figure 10 show the abundances of meteoritic elements in the average of the Wanapitei melts compared to abundances in the LL-, L-, H-, and C1-chondrites. The plot includes Au, Ge, Se uncorrected and shows the trends for chondrites and the Wanapitei melt rocks. Figure 11 shows ratios of meteoritic elements in chondrites versus Wanapitei data. The general trend for the Wanapitei rocks is consistent with the whole group of chondrites. The anomalous cobalt offsets the Ni/Co and Cr/Co ratios. This fact had been previously noted by Wolf et al. (1980). The researchers suggested the possibility of a secondary source of cobalt in the area to explain its concentration levels. Figure 12 presents the C1 normalized pattern for the Wanapitei samples and LL-chondrites. The plot is made for the same elements as presented by Wolf et al. (1980), and shows the Wanapitei trend being consistent with the group of chondrites. From the data presented in Figures 11, 12 and Table 11, however, it appears, that none of the presented types of chondrite matches exactly the Wanapitei data. Thus, it cannot be confirmed whether an LL-chondrite (as suggested by Wolf et al., 1980) is the type of projectile recorded in the Wanapitei impact

rocks. Identification of the projectile proposed by Wolf et al. (1980) was largely based on matching the Ni/Cr ratios in three samples of impact lithologies with chondrite data. This study considers broader data, and the results are repeatable (Table 11); however, due to the "statistical" character of many of them (mixing model results, mean compositions of rocks, etc.), a coincidence cannot be excluded.

The differences in compositional trends between chondrites and meteoritic content of Wanapitei rocks which occur, e.g., for Co, Cr, Pd (Figure 12) or Re (Figure 10), can generally result from several factors:

-heterogeneous distribution of the meteoritic elements within the melts

-fractionation during the impact, or partial to complete volatilization (Au, Ge and Se depletion in impact rocks, Table 9)

-redistribution of volatile elements during cooling of the melt sheet and/or loss of them from its top layer

-fractionation during weathering (Re, Figure 10)

-the hydrothermal sulphide mineralization, known from the Wanapitei Lake area (Dressler, 1982), could have influenced the element content (Au, Ni, Pd)

-hydrothermal remobilization of Au, or removal of Au and Re by aqueous solutions, could take place on cooling of the melts, as was suggested for Brent crater, Ontario (Grieve, 1978). The

average degree of the meteoritic contamination of impact melts has been estimated at 1-2% of the C1 type of chondrite equivalent (Palme et al., 1978 and 1980; Göbel et al., 1980; Wolf et al., 1980). In case of lithologies of the Wanapitei crater in which the meteoritic signal is strong, the contamination levels range from less than 0.5% to about 1.5%.

Table 9. Meteoritic content of Wanapitei impact melt rocks.

| | Wanapitei uncorrected | Target rocks indigeneous | Wanapitei meteoritic content |
|---|---|---|---|
| Co (ppm) | 13.30 | 6 | 7.30 |
| Cr (ppm) | 54.60 | 25 | 29.60 |
| Ni (ppm) | 95.60 | 23 | 72.60 |
| Os (ppb) | 2.10 | 0.20 | 1.90 |
| Ir (ppb) | 2.33 | 0.04 | 2.29 |
| Pd (ppb) | 3.42 | 2.55 | 0.87 |
| Au (ppb) | 4.59 | 16.03 | n/a |
| Ge (ppb) | 921 | 985.50 | n/a |
| Se (ppb) | 11.40 | 17.75 | n/a |
| Re (ppb) | 0.106 | 0.07 | 0.036 |

*Target rocks data from Table 8, adding 56.4% of Mississagi Fm. to 43.6% of Gowganda Fm., except for Cr, Au, Ge, Se, Re.

*Co, Cr, and Ni uncorrected data are mean of 14, 11 values from Table 2 and 3 from Table 3.

*Os to Re uncorrected data from Table 3.

Table 10. Meteoritic element abundances in chondrites and Wanapitei impact melt rocks.

| | Type of chondrite | | | | | | | | | Wanapitei |
|---|---|---|---|---|---|---|---|---|---|---|
| | LL | L | H | CI | CM | CO | CV | EH | EL | |
| Cr (ppm) | 3740 | 3880 | 3660 | 2650 | 3050 | 3550 | 3600 | 3150 | 3050 | 29.6 |
| Co (ppm) | 490 | 590 | 810 | 508 | 575 | 688 | 655 | 840 | 670 | 7.3 |
| Ni (ppm) | $10.2x10^3$ | $12x10^3$ | $16x10^3$ | $10.7x10^3$ | $12x10^3$ | $14x10^3$ | $13.4x10^3$ | $17.5x10^3$ | $13x10^3$ | 72.6 |
| Ge (ppm) | 9 | 10 | 13 | 33 | 23 | 21 | 17 | 42 | 28 | 0.921 |
| Se (ppm) | 10 | 9 | 8 | 20 | 13 | 8 | 8 | 26 | 14 | 11.4 |
| Pd (ppb) | 530 | 560 | 870 | 560 | 640 | 703 | 705 | 885 | 690 | 0.87 |
| Os (ppb) | 400 | 515 | 820 | 490 | 640 | 790 | 825 | 654 | 589 | 1.9 |
| Au (ppb) | 140 | 162 | 215 | 144 | 185 | 184 | 144 | 330 | 225 | 4.59 |
| Ir (ppb) | 360 | 490 | 760 | 460 | 595 | 735 | 760 | 585 | 525 | 2.29 |
| Re (ppb) | 33 | 40 | 70 | 37 | 46 | 55 | 65 | 52 | 47 | 0.036 |
| Nb (ppb) | 370 | 390 | 360 | 270 | 370 | 450 | 540 | 250 | - | 8 |
| Rb (ppm) | 3.1 | 3.1 | 2.9 | 2.22 | 1.7 | 1.45 | 1.25 | 2.6 | 2.5 | 64 |

*Wanapitei data corrected for indigeneous content, except for Au, Ge, Se, Nb, and Rb (Table 9).

*Chondrites data from Wasson et al. (1988).

Table 11. Element ratios in chondrites and in Wanapitei impact melt rocks.

| Element ratio | Type of chondrite | | | | | | | | | Wanapitei |
|---|---|---|---|---|---|---|---|---|---|---|
| | LL | L | H | CI | CM | CO | CV | EH | EL | |
| Ni/Ir | $28x10^3$ | $24.5x10^3$ | $21.1x10^3$ | $23.3x10^3$ | $20.2x10^3$ | $19.1x10^3$ | $17.6x10^3$ | $31x10^3$ | $24.8x10^3$ | $31.7x10^3$ |
| Ni/Co | 20 | 20.3 | 19.8 | 21.1 | 20.9 | 20.3 | 20.5 | 20.8 | 19.4 | 9.9 |
| Cr/Co | 6.6 | 6.6 | 4.5 | 5.2 | 5.3 | 5.2 | 5.5 | 3.8 | 4.6 | 4.1 |
| Cr/Ir | $11x10^3$ | 7918 | 7469* | 5761 | 5126 | 4830 | 4737 | 5575 | 5810 | $12.9x10^3$ |
| Ni/Cr | 2.5 | 3.1 | 4.4 | 4.0 | 3.9 | 3.9 | 3.7 | 5.6 | 4.3 | 2.5 |
| Co/Ir | 1400 | 1204 | 1066 | 1104 | 966 | 936 | 862 | 1487 | 1276 | 3188 |

*Chondrite data from Wasson et al. (1988).

*Wanapitei data from Table 3 and 10.

Figure 10. Element abundances in chondrites compared with Wanapitei impact melt rocks.

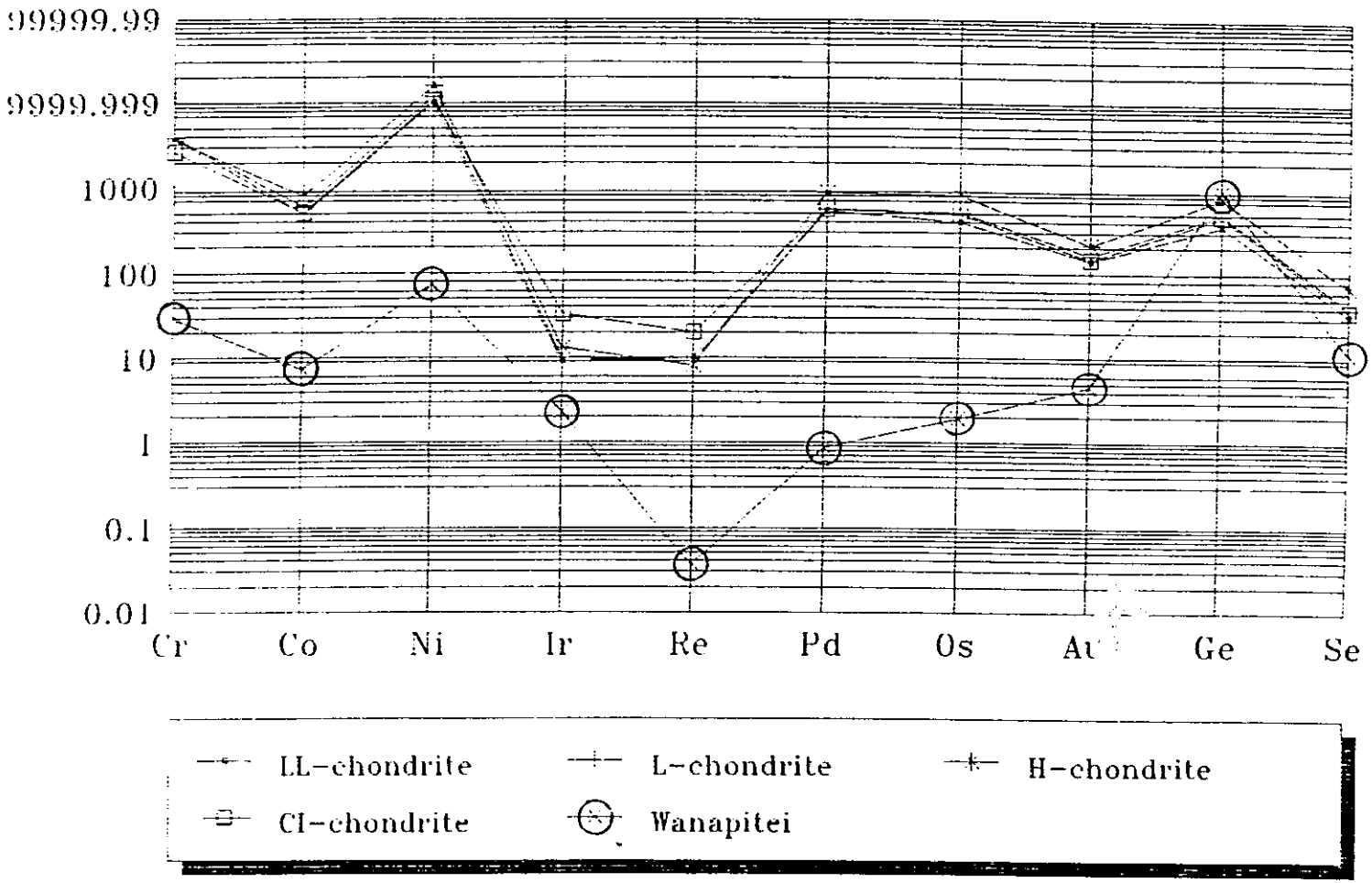


Data from Table 3 and 9.

Figure 11. Chondritic element ratios compared with Wanapitei impact melt rocks ratios.

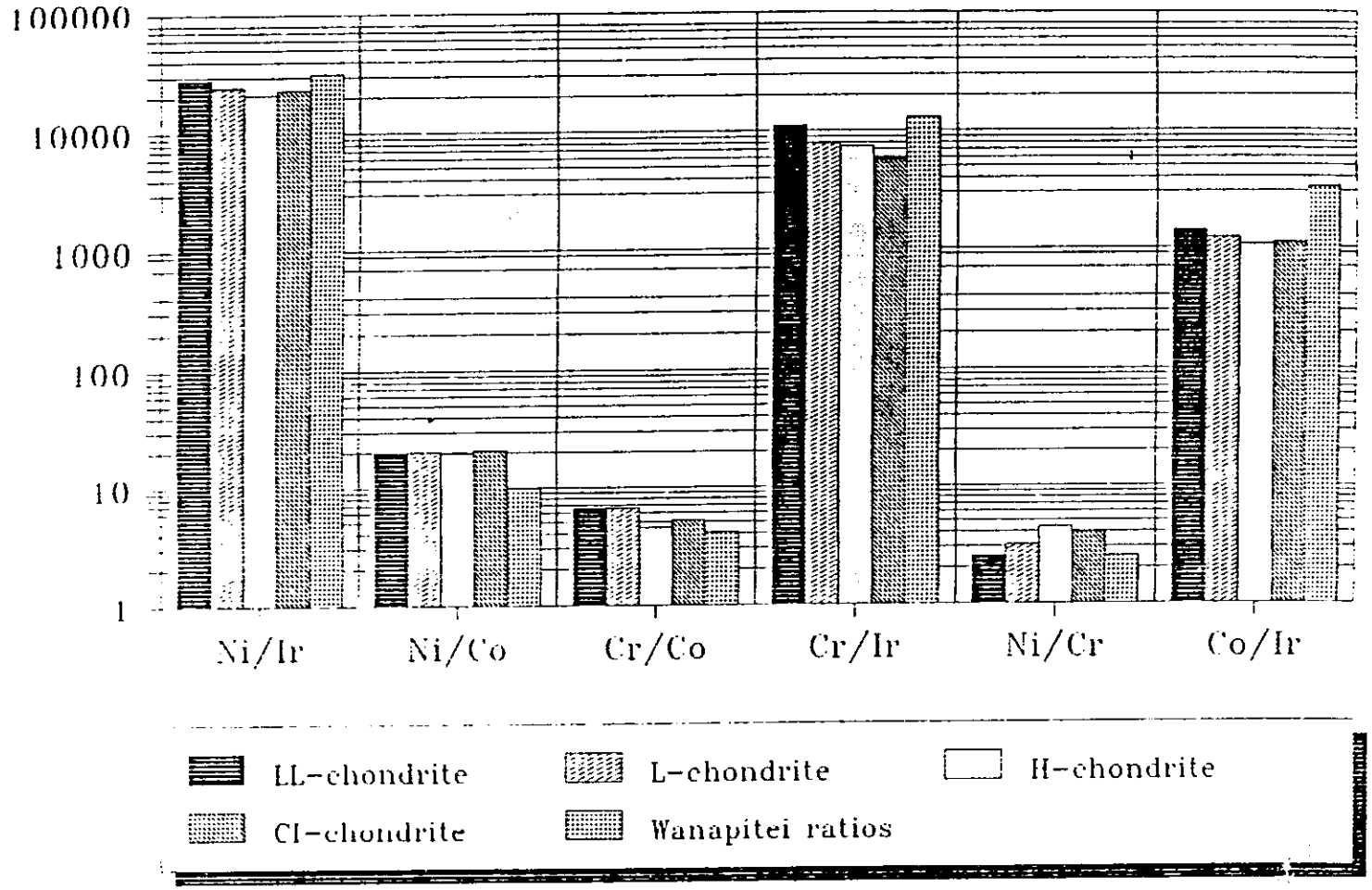


Data from Table 11.

Figure 12. The meteoritic pattern at Wanapitei impact melt rocks.

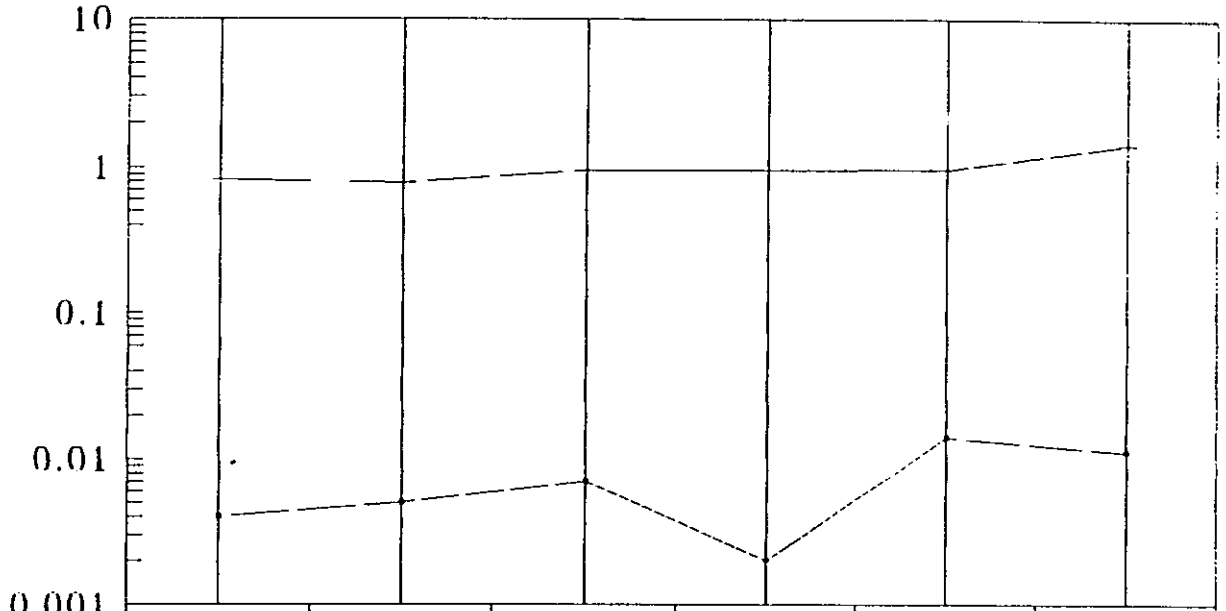


| | Os | Ir | Ni | Pd | Co | Cr |
|---|---|---|---|---|---|---|
| Wanapitei/CI | 0.004 | 0.005 | 0.007 | 0.002 | 0.014 | 0.011 |
| LL-chondrite/CI | 0.82 | 0.78 | 0.95 | 0.95 | 0.96 | 1.41 |

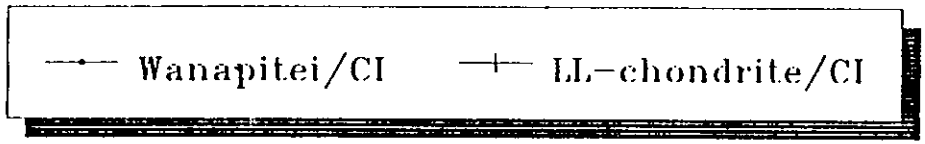

## Discussion of the Results

The present study has enhanced the existing database for the Lake Wanapitei impact structure by contributing:

-Microscopic examination of shocked rocks collected from the southern margin of Lake Wanapitei.

-XRF and microprobe analyses of these rocks.

-Mixing model calculations to determine relationship between the shocked and country rocks, which enabled:

-Determination of lithological composition of the target area at the time of impact.

-Description and classification of shock metamorphic features recorded in the Wanapitei crater lithologies, including analysis of planar features in quartz using a universal stage.

-Estimate of pressure and temperature conditions of the impact.

-Model of distribution of the shock metamorphic features within the Wanapitei crater.

Several conclusions arise regarding the Wanapitei impact event. The results of chemical and microprobe analyses, combined with the mixing model calculation, indicate that the average melt rock was generated from 56% average Mississagi Formation and 44% average Gowganda Formation, implying that at the time of the Wanapitei impact, the sediments of the two formations dominated

the surficial geology in the area. The impact-induced changes recorded in the Wanapitei crater lithologies represent virtually all grades of shock metamorphism. Due to lack of geological data regarding the submerged part of the Wanapitei Lake depression, it is difficult to assess the level of participation of other lithological units in the formation of the impact structure. The Archean gneisses which have been moderately shocked must be regarded as part of the target area. However, from the grade of shock metamorphism observed in those rocks and their local geological setting, it appears that the Wanapitei impact did not affect those units as strongly, and as "directly", as it did with the Huronian quartzitic sedimentation. Possibly at that time, the Archean gneisses formed a southwesterly trending zone, which did not extend as far to the north as at present. Thus, they were in the peripheral margin of the shock range. Also, the level of participation of the Nipissing Intrusives and the Late Precambrian olivine diabase dikes in the impact melt rocks is none, or undetected. The mixing model rejected both of these as the "candidates"; however, this result alone cannot be decisive (see note on p.65). Their random distribution within the Huronian sediments (Figure 1) suggests, that the probability of the dikes being present in the central and marginal parts of the target area is approximately 0.01. In the past, the Nipissing Intrusives were regarded as the contributors of the minor mafic content to the impact melt rocks (Winzer et al., 1976). The

present study does not support this view. The precise identification of source of the mafic content is needed to better understand the composition of target area for the Wanapitei structure. Future work on the subject could be focused on creating a mixing model from a larger set of data on country rocks. The data should come from samples collected from the outcrops adjacent to the Wanapitei structure. Possibly, the new model could closer define composition of the target area. It would also show the extend and influence of compositional variations of the country rocks on results of the mixing model calculations.

From the available data on the crater lithologies, five main groups of impact related rocks have been identified according to the shock metamorphic features observed in them. The impact breccias, shocked gneiss, shocked sediments with glass, suevites, and vesicular glassy melt rocks display a systematic sequence of shock deformations. It is, however, understood that the available suite of shocked rocks from the Wanapitei structure may not be complete; thus, future investigations may introduce modifications to the proposed classification. The shock metamorphic deformations recorded in the Wanapitei impact rocks include fracturing, mineral kinking, planar features in quartz, ballen quartz, diaplectic glass of quartz and plagioclase (maskelynite), fused glasses, and high pressure polymorphs of $SiO_2$, i.e. coesite and lechatelierite (Dence and

Popelar, 1972 and Dence et al., 1974). The schematic model of distribution of shock zones of shock metamorphism (Figure 6) has been derived from the record of continuous stages of shock deformations in quartz and previous attempts at other impact craters (Stöffler, 1966 and 1971; Engelhardt and Stöffler, 1968; Lakomy, 1990a&b; Dressler, 1990). Based upon the analysis of these features, the peak recorded conditions of the Wanapitei event were pressures of approx. 70 GPa and temperatures of up to ~2500°C. The scale of the Wanapitei event generated pressures and temperatures high enough to melt and vaporize the meteorite.

The meteoritic enrichment of the impact melt rocks is quite well preserved in the original fixed meteoritic ratios (Figure 11). The level of contamination of the Wanapitei shocked rocks reaches up to 1.5% of meteoritic material, which represents a relatively strong chemical signature of the projectile. The enrichment-depletion patterns of the meteoritic elements for the Wanapitei melt rocks (Figures 10 and 12) partially confirm previous accounts by Wolf et al. (1980), identifying LL-chondrite as the type of projectile involved in the impact event. However, from the data acquired in this study, it is impossible to point to the specific type of chondrite involved.

## APPENDIX A. The Wanapitei Crater Lithologies.

Presented here is the petrographic description of eleven samples of shocked rocks recovered from glacial float south of the village of Skead (Figure 1). The samples represent the varieties of the Wanapitei crater lithologies.

**1) WTB-2T-90 : Vesicular glassy melt rock with shocked quartz.**

The freshly obtained surface of the rock is grey to light grey with low lustre, flow texture and vesicles. Despite the presence of the flow texture, the vesicles are very well-rounded non-oriented spherules up to 1.5 cm in diameter.

In thin section, the sample comprises fresh vesicular glass matrix, inclusions of quartz and minor feldspar (Plate VI). The glass is colourless and optically homogeneous, with patches of fine devitrified material and perlitic cracks. The vesicles are well rounded, mostly spherical, surrounded by devitrified cryptocrystalline zones of silica. Feldspars in matrix are plagioclase laths in two distinctive "size-sets". The fine (on average 0.1 mm long) crystallines "emerge" from the glass as a quench plagioclase. The coarser fractions could originate from slower devitrification. Some of the plagioclases are concentrated in radial and variolitic assemblages.

Quartz clasts vary in concentration, accounting for up to 25% of the rock. The main varieties include: ballen quartz (subconchoidally fractured from thermal stress; Lehtinen, 1976,

p.26), shocked quartz with planar features, minor diaplectic glass, and unshocked quartz. The planar features were observed in up to three sets of ω-{10$\bar{1}$3}, two sets of ω-{10$\bar{1}$3}&π-{10$\bar{1}$2}, ω-{10$\bar{1}$3}&ω-{10$\bar{1}$3}, ω-{10$\bar{1}$3}&c-{0001}, and single sets of ω-{10$\bar{1}$3}, or a-{11$\bar{2}$0} type-D deformations (graphical presentation of their frequency versus angles to c-axis combined for all measurements is given in Figure 5; detailed discussion of the deformations is given in the conclusions chapter). The quartz inclusions are subrounded to rounded. Most of the grains are fractured and have boundaries made of fine "collars" of devitrified silica.

**2) WTB-2-2RA : Vesicular glassy melt rock with shocked quartz.**
The fresh surface is light grey with yellowish phenocrysts, with a very low lustre. Vesicles and fractures are common. The rock is of low density.

In thin section, the sample contains vesicular glass matrix with feldspars, and quartz inclusions (Plate VII). The glass is homogeneous without flow textures, with approximately 50% of it recrystallized into feldspars. The feldspar, mainly plagioclase, form a regular network of minute laths averaging 0.1 mm in length. The vesicles are rounded and have boundaries made of fine devitrified silica material. Quartz occurs in a variety of inclusions, among which the ballen and fractured types are dominant. The shocked grains with planar features are minor. The

planar features form up to two sets of ω-{10$\bar{1}$3}&ω-{10$\bar{1}$3}, π-{10$\bar{1}$2}&c-{0001}, π-{10$\bar{1}$2}&ω-{10$\bar{1}$3}, and single sets of ω-{10$\bar{1}$3}, and m-{10$\bar{1}$0} deformations. The features are "decorated", cutting through the irregular fracturing. The quartz grains are rounded to subrounded, moderately embayed with minor content of diaplectic glass. The total quartz accounts for 15-25% of the rock. Unidentified minor lithic fragments of mafic rocks with thick alteration aureoles were observed.

**3) WTB-2A-2F : Vesicular glassy melt rock with shocked quartz.**
The fresh surface is vesicular, brown to white, with low lustre. Flow textures are noticeable, forming a characteristic lineament.

In thin section, it is composed of brown glass, colourless glass, quartz inclusions, and lithic fragments (Plate IX). The glasses are intermixed, displaying a characteristic flow texture. The vesicles in both glasses are elongated toward the direction of flow. Most of the vesicles display very thin, devitrified silica rims on their boundaries. The glasses are partially recrystallized to a very fine feldspathic material. Quartz inclusions and lithic fragments are coarse to fine, angular to rounded; some are strongly embayed or fractured. The observed varieties include ballen quartz, quartz with multiple irregular fractures, and shocked quartz with single sets of ω-{10$\bar{1}$3}, ξ-{11$\bar{2}$2}, c-{0001}, π-{10$\bar{1}$2}, or s-{11$\bar{2}$1} decorated

planar features. Some of the ballen quartz grains display patches of diaplectic glass in the central zones of the grains. Lithic clasts form 2-5% of the rock. They are strongly altered, and thus are difficult to recognize. Mostly quartzitic, gabbroic, and diabase fragments were recognized.

**4) WTB-2-2C : Vesicular glassy melt rock with shocked quartz.**

The rock is dark grey, with medium lustre and regular spherical vesicles, despite the evident lineament from flowing.

In thin section, the sample comprises vesicular glass matrix, feldspars ,and quartz (Plate VIII). The glass is colourless, with dense perlitic cracks. The vesicles vary in size but all are rounded, with relatively thin devitrified silica zones on boundaries. Feldspars in the matrix, mostly plagioclases, are fine quench crystallines and coarser slowly devitrified phases sporadically organized in variolitic assemblages. Both account for up to 45% of the matrix. Quartz inclusions are randomly distributed throughout the entire rock. They are fine to coarse, subangular to rounded, some with dense fractures. Most of them are ballen quartz and deformed grains with single sets of ω-$(10\bar{1}3)$, s-$(11\bar{2}1)$, or a-$(11\bar{2}0)$ planar features. Some inclusions are strongly embayed and display patches of diaplectic glass.

**5) WTB-3S-90 : Suevite breccia with shocked quartz.**

The rock is dark brown and comprises a variety of clastic

fragments set in fragmental matrix. The clasts are subrounded to rounded and are mostly of quartz. The rock breaks apart with relative ease.

In thin section, the sample contains lithic clasts, quartz, feldspar, and fragmental glassy matrix (Plate V). The lithic clasts range in size from less than 0.5 mm to several cm in diameter. They are subangular to angular, moderately to intensely fractured. The identified lithic types were: sandstone, siltstone, argillite, glassy melt, wacke, and diabase in fragments up to several cm in diameter. Glassy fragments are subangular to angular, with high vesiculation and a brown colouring. Quartz grains range from approx. 0.1 mm to approx. 0.75 cm in diameter, and are angular to subrounded. The deformed grains were observed to have up to three sets of decorated or nondecorated planar features per grain. The single sets are represented by the $\omega$-$\{10\bar{1}3\}$, or m-$\{10\bar{1}0\}$ type-C deformations. The double sets comprise the $\omega$-$\{10\bar{1}3\}$ or z-$\{01\bar{1}1\}$ with $\omega$-$\{10\bar{1}3\}$ deformations. Other type-D deformations are $\pi$-$\{10\bar{1}2\}$ in triple sets with the $\omega$-$\{10\bar{1}3\}$.

Feldspars, mostly plagioclases, are similar in size and shape to the quartz, with minor kinking and maskelynite. The fine fractions of all of the constituents form up to 40% of fragmental matrix. Vesicular glass and a nonrecognizable cryptocrystalline phase account for the remainder. The glass is brownish to colourless with vesicles. Some of the vesicles and

clasts have oxidized boundaries.

**6) WTB-2-2G : Vesicular glassy melt rock.**

The fresh surface is dark grey with yellowish vesicles and low lustre. Vesicles are elongated and, together with the characteristic lineament, form an oriented flow texture. The mineral phases are fine grained, and light in colour.

In thin section, the sample comprises vesicular glass with minor feldspars, inclusions of quartz, and lithic fragments (Plate X). The glass is colourless to light brown, partly devitrified into a very fine silica and feldspars. Vesicles are common, varying in shape and size. Most of them are oval with prevailing orientation and with thin devitrified zones on boundaries. Rare oval cavities (Plate X) contain numerous fragments of glass, lithic clasts, quartz, and feldspars. Quartz inclusions are randomly distributed throughout the glass. They are fine to medium, subrounded to rounded, weakly to strongly fractured. Clusters of quartz grains quite common account for 2-5% of the mode. Ballen quartz constitutes up to 50% of the total quartz, often displaying a minor content of diaplectic glass. Lithic clasts are medium to coarse, subrounded to rounded. Those recognized were sandstone, siltstone, and diabase. Plagioclase grains, form up to 2% of the rock. They are fine to medium subrounded to rounded, fractured with characteristic sericitization. No planar features were observed in this sample.

**7) WTB-2-2X : Vesicular glassy melt rock.**

The fresh surface of the rock is homogeneous, grey to light brown, with low lustre and rounded vesicles. The vesicles are up to ~1.0 cm in diameter. Fine, light coloured, mineral inclusions are noticeable. No flow textures were observed.

In thin section, the sample contains vesicular glass, quartz and feldspars (Plate XI). The glass is colourless and optically homogeneous with perlitic cracks. It accounts for 75-95% of the mode. The vesicles in glass are rounded, variable in size (max. ~1.0 cm in diameter). Most of them are partially or entirely filled with layered microcrystalline silica (Plate XI). Less than 50% of the glass is devitrified into a very fine plagioclase laths. The other, minor plagioclases are coarser and have blade-type crystals. The quartz inclusions commonly display tension fractures or ballen character. Ballen quartz is often embayed and attached or surrounded by assemblages of microcrystalline silica. Such clusters account for 2-3% of the rock. No planar features in quartz were observed in this sample.

**8) WTB-2-2F : Shocked quartzitic sediment with glass.**

The rock has a low density and breaks apart easily. A very fine vesiculation is noticeable. No flow textures were observed on the grey to yellowish surface.

Thin section examination reveals that the sample contains quartz

inclusions and vesicular glass (Plate IV). Quartz inclusions account for at least 70% of the rock. It is fractured and partially melted along the grain boundaries and the fractures. Some of the fractures are irregular; others represent curvilinear mosaics observed in ballen quartz. The interstitial glass is partially devitrified to cryptocrystalline silica. Numerous quartz grains display diaplectic glass, in part or entirely. The glass is brownish to colourless. Irregular in size and shape vesicles occupy intergranular spaces between the quartz inclusions. No planar features were seen in this sample.

**9) WTB-2A-2E : Vesicular glassy melt rock.**

The fresh surface is dark grey with white to yellowish inclusions. Vesicles are spherical, randomly distributed, up to ~0.75 cm in diameter.

In thin section, the sample comprises vesicular glass, inclusions of quartz, and feldspars (Plate XII).

The glass is optically homogeneous with perlitic cracks and rounded vesicles of various sizes. Some of them display devitrified silica zones on their boundaries. The glass does not show any flow textures. Quartz is present as oval shaped inclusions randomly distributed in the rock and reaching up to 1.0 mm in diameter. The most abundant, ballen quartz and a "regular" quartz are weakly to strongly fractured. The ballen type displays diaplectic glass in central zones of the grains.

Feldspars are present as laths of plagioclases quenched from the glass. Most of the larger, blade-like grains are organized in radial patterns. Thinner crystallites form "thick" variolitic assemblages. They account for up to 30% of the mode. No planar features were found in this sample.

**10) WTB-2-2M : Vesicular glassy melt rock.**

The fresh surface is light brown to grey with few lighter patches. The abundant vesicles are rounded to oval displaying orientation. The rock is fractured, and breaks apart with ease. In thin section, the sample consists of vesicular glass and quartz (Plate XIII). The silica glass is light brown to colourless, optically homogeneous, without flow textures. Approximately 10% of the glass has undergone devitrification into the fine feldspathic crystallines. The quartz inclusions measure up to 1.5 mm in diameter. They are mostly single grains among which the ballen and randomly fractured quartz are the main types. The ballen type is rich in diaplectic glass and often embayed. The distribution of quartz is variable and may reach from 10 to 50% of the mode. Planar features were not found in this sample.

**11) WTB-2-2U : Polymict glassy breccia.**

The rock is of low density. The freshly broken surface is light brown to grey. Lithic fragments and quartz grains are partly

recognizable, varying in size from very fine to several cm in diameter and up to ~1.0 mm, respectively. Most of them are subrounded to rounded. Vesicles form irregular and elongated voids without defining a flow texture.

In thin section, the sample contains fragments of vesicular glass, lithic fragments, and quartz grains set in a fragmental matrix (Plate III). The glass fragments are angular with flow textures, varying in colour from brown to colourless. Some of the fragments contain inclusions of quartz, diaplectic quartz glass, and lithic clasts of quartzitic sediments, all of which are moderately fractured. Other lithic fragments in the breccia are siltstone, sandstone, quartzite, diabase, wacke, argillite, and strongly altered gabbroic rock. Their size and shape range from minute inclusions in the matrix to clastic fragments ~2 cm in diameter, and from angular to rounded, respectively. Quartz grains are angular to rounded, from less than 0.1 mm to ~1.0 mm in diameter. There are no ballen quartz or grains with planar shock features. Feldspars are present, but not abundant, constituting 1-3% of the mode and are mostly represented by finely sericitized plagioclases. The matrix contains all of the lithic and clastic constituents, with noticeable domination of quartz set in a glassy partially recrystallized material.

**12) MSWX-119-70: Shocked granitic gneiss.**

Thin-section examination reveals rock of gneissic texture. Most

mineral grain sizes average ~1.0 mm in diameter. The main constituents are quartz (~40% of the mode), feldspars (~35% of the mode), and mafic minerals (~15% of the mode). Muscovite and glass account for the remainder. Quartz in this sample displays no planar features; however, approx. 10% of it is recrystallized into microcrystalline aggregates which preserve original fracturing and grain boundaries. Feldspars are represented mostly by plagioclases displaying twin kinking and sericitization. Mafic minerals (pyroxenes and amphiboles) are strongly altered and difficult to recognize. Minor phases in the rock are muscovite and glass. The glass is brown to mixed and of interstitial character. The clear type was not observed. The glass is mostly concentrated around mafic constituents, in places displaying incipient crystallization of pyroxene. No flow textures or vesicles were observed. Twin kinking in plagioclase, and strong fracturing of the rock could originate due to weak (several GPa) shock metamorphism. However, the glass very likely formed later, during the slower phase of cooling of the rock associated with thermal annealing processes.

## APPENDIX B. Glossary

Apparent crater - fully developed crater with features such as rim, impact breccia, and melt rock sediments.

Ballen quartz - the annealing product after diaplectic quartz glass.

Coesite - high pressure polymorph of $SiO_2$.

Diaplectic glass - glass formed without melting.

Fused glass - glass formed from a liquid phase.

Lechatelierite - amorphous $SiO_2$ originated under extremely high pressure and temperature, often observed as characteristic sinusoidal and curvilinear concentrations from cooling.

Maskelynite - diaplectic glass of plagioclase composition.

Stishovite - high pressure polymorph of $SiO_2$.

Suevite - breccias containing a variety of shock metamorphosed rock fragments.

Transient crater - impact excavated cavity excluding impact-induced slumping, faulting, and fall-back sedimentation.

**REFERENCES:**

Ahrens, T.J., Rosenberg, J.T., 1968. Shock metamorphism: Experiments on quartz and plagioclase, in Shock metamorphism of natural materials, French, B.M., Short, N.M., eds., Mono Book Corp., 1968, p.59-81.

Beals, C.S., Dence, M.R., Cohen, A.J., 1967. Evidence for the impact origin of Lac Couture. Publ. Dom. Obs., v.31, 10, p.411-426.

Bell, R., 1891. Report on the Sudbury Mining District. Geological Survey of Canada, Annual Report,v.5, Part 1, 1890-91, Report F, p.1-95.

Bunch, T.E., 1968. Some characteristics of selected minerals from craters, in Shock metamorphism of natural materials, French, B.M., Short, N.M., eds., Mono Book Corp., Baltimore, p.413-432.

Card, K.D., 1978. Geology of the Sudbury-Manitoulin area, districts of Sudbury and Manitoulin. Ontario Geological Survey, Report 166, 238p., Accompanied by Map 2360 and 4 charts.

Card, K.D., Innes, D.G., Debicki, R.L., 1977. Stratigraphy, sedimentology, and petrology of the Huronian Supergroup in the Sudbury-Espanola area. Ontario Division of Mines, Geoscience Study 16, 99p., Accompanied by 4 charts.

Chao, E.C.T., 1968. Pressure and temperature histories of shock metamorphosed rocks-based on petrographic observations, in Shock metamorphism of natural materials, French, B.M., Short, N.M., eds, Mono Book Corp., p.135-158.

Chesnokov, B.V., Popov, V.A., 1965. Increase in the volume of quartz grains in south Urals eclogite. Doklady Akademiia Nauk SSSR, 162, p.176-178.

Chopin, C., 1984. Coesite and pure pyrope in high-grade blueschists of the Western Alps: A first record and some consequences. Contrib. Mineral. Petrol., 86, p.107-118.

Collins, W.H., 1913. Geology of a portion of Sudbury Map-Area, south of Lake Wanapitei, Ontario. Geological Survey of Canada, Summary Report for 1913.

Dence, M.R., Popelar, J., 1972. Evidence for an impact origin for Lake Wanapitei, Ontario, in New developments in Sudbury geology, Guy-Bray, J.V., ed., Geological Association of

Canada, Special Paper 10, p.117-124.

Dence, M.R., Robertson, P.B., Wirthlin, R.L., 1974. Coesite from the Lake Wanapitei crater, Ontario. Earth Planet. Sci. Letters, v.22, p.118-122.

Dence, M.R., Grieve, R.A.F., Robertson, P.B., 1977. Terrestrial impact structures: principal characteristics and energy considerations, in Impact and explosion cratering, Roddy, D.J., Pepin, R.O., Merrill, R.B., eds., Pergamon Press, New York, p.247-275.

Dressler, B.O., 1982. Geology of the Lake Wanapitei area, District of Sudbury. Ontario Geological Survey, Report 213, 131p.

Dressler, B.O., 1984. General geology of the Sudbury area, in The geology and ore deposits of the Sudbury structure, Pye, E.G., Naldrett, A.J., Giblin, P.E., eds., Ontario Geological Survey, Special Volume 1, p.57-82.

Dressler, B.O., 1990. Shock metamorphic features and their zoning and orientation in the Precambrian rocks of the Manicouagan Structure, Quebec, Canada. Tectonophysics, 171, p.229-245.

Duvall, G.E., Graham, R.A., 1977. Phase transitions under shock-wave loading. Rev. Mod. Phys., 49, p.523-579.

Enami, M., Zang, Q., 1990. Quartz pseudomorphs after coesite in eclogites from Shandong province, east China. Amer. Miner., v.75, p.381-386.

Engelhardt, W., Stöffler, D., 1968. Stages of shock metamorphism in crystalline rocks of the Ries Basin, Germany, in Shock metamorphism of natural materials, French, B.M., Short, N.M., eds., Mono Book Corp.

Fairbairn, H.W., Hurley, P.M., Card, K.D., Knight, C.J., 1969. Correlation of radiometric ages of Nipissing diabase and Huronian metasediments with Proterozoic orogenic events in Ontario. Can. Jour. Earth Sci., v.6, p.489-497.

Frarey, M.J., Roscoe, S.M., 1970. The Huronian Supergroup north of Lake Huron, in Symposium on basins and geosynclines of the Canadian shield, Baer, A.J., ed., Geological Survey of Canada, Paper 70-40, p.143-157.

Gary, M., McAfee Jr., R., Wolf, C.L., eds., 1973. Glossary of Geology. Amer. Geol. Institute, Washington, D.C.

Gates, F.M., Hurley, P.M., 1973. Evaluation of Rb-Sr dating method applied to the Matachewan, Abitibi, Mackenzie, and Sudbury Dike Swarms in Canada. Can. Jour. Earth Sci., v.10, p.900-919.

Gibbins, W.A., McNutt, R.H., 1975. Rubidium-Strontium mineral ages and polymetamorphism at Sudbury, Ontario. Can. Jour. Earth Sci., v.12, p.1990-2003.

Göbel, F., Reimold, U., Baddenhausen, H., Palme, H., 1980. The projectile of the Lappajarvi crater. Z. Naturforsch, 35a, p.197-203.

Grieve, R.A.F., 1978. The melt rocks at Brent crater, Ontario. Proc. Lunar Planet Sci. Conf., 10th, p.2535-2545.

Grieve, R.A.F., 1987. Terrestrial impact structures. Ann. Rev. Earth Planet. Sci., 15, p.245-270.

Innes, M.J.S., Pearson, W.J., Geuer, J.W., 1964. The Deep Bay crater. Publ. Dom. Obs., v.31, 2, p.19-52.

Janssens, M-J., Hertogen, J., Takahashi, H., Anders, E., 1977. Rochechouart meteoritic crater: Identification of projectile. Jour. Geoph. Res., v.82, 5, p.750-758.

Junnila, R.M., 1990. Precambrian geology, Yarrow and Doon Townships with emphasis on the Huronian Supergroup. Ontario Geological Survey, Report 277, 33p.

Koulomzine, T., 1955. Unpublished report on Dolmac Mines Limited property, Rathbun Township, district of Sudbury. File 63-6035, Assessment File Research Office, Ontario Geological Survey, Ministry of Natural Resources, Toronto.

Lakomy, R., 1990a. Distribution of impact induced phenomena in complex terrestrial impact structures. Implications for transient cavity dimensions. Abstract, Lunar Planet. Sci., XXI, p.676-677.

Lakomy, R., 1990b. Implications for cratering mechanics from breccias of the Sudbury impact crater, Canada. Abstract, Lunar Planet. Sci., XXI, p.678-679.

Lehtinen, M., 1976. Lake Lappajärrvi, a meteorite impact site in western Finland. Geological Survey of Finland, Bulletin, 282, 92p.

Melosh, H.J., 1989. Impact cratering. A geological process. Oxford Monographs on Geology and Geophysics, 11, Oxford University Press, 245p.

Meyn, H.D., 1970. Geology of Hutton and Parkin Townships. Ontario Department of Mines, Geological Report 80, 78p., Accompanied by Map 2180.

Mirwald, P.W., Massonne, H.J., 1980. Quartz-coesite transition and the comparative friction measurements in piston-cylinder apparatus using talc-alsimag-glass (TAG) and NaCl high pressure cell. A discussion, Neues Jahrbuch für Mineralogie Monatshefte, p.469-477.

Morgan, J.W., Higuchi, H., Ganapathy, R., Anders, E., 1975. Meteoritic material in four terrestrial impact craters. Proc. Lunar Sci. Conf., 6th, p.1609-1623.

Murray, A., 1853-56. Report of progress. Geological Survey of Canada, 101p.

Ogden, M., 1957. Unpublished report on Dolmac Mines Limited property, Rathbun Township, district of Sudbury. File 64-6035, Assessment File Research Office, Ontario Geological Survey, Ministry of Natural Resources, Toronto.

Ogilvie, B.Y., Robertson, P.B., Grieve, R.A.F., 1984. Meteorite impact features in Canada: An inventory and an evaluation. Unpublished paper available from Geophysics Division,

Geological Survey of Canada, Ottawa.

Palme, H., Janssens, M-J., Takahashi, H., Anders, E., Hertogen, J., 1978. Meteoritic material at five large impact craters. Geochim. Cosmochim. Acta., v.42, p.313-323.

Palme, H., 1980. The meteoritic contamination of terrestrial and lunar impact melts and the problem of indigenous siderophiles in the lunar highlands. Proc. Lunar. Planet. Sci. Conf., 11th, p.481-506.

Popelar, J., 1971. Gravity measurements in the Sudbury area: Canada Department of Energy, Mines and Resources, Earth Physics Branch, Gravity Map Series, 138.

Pye, E.G., Naldrett, A.J., Giblin, P.E., eds., 1984. The geology and ore deposits of the Sudbury structure. Ontario Geological Survey, Special Volume 1, 603p. Accompanied by Map 2491, at a scale of 1:50 000, Map NL-16/17-AM Sudbury, at a scale of 1:1 000 000, and 3 charts.

Robertson, P.B., Dence, M.R., Vos, M.A., 1968. Deformations in rock forming minerals from Canadian craters, in Shock metamorphism of natural materials, French, B.M., Short, N.M., eds., Mono Book Corp., 1968, p.433-452.

Robertson, P.B., Grieve, R.A.F., 1975. Impact structures in Canada: Their recognition and characteristics. R. Astr. Soc. Can. Jour., v.69, 1, p.1-20;

Robertson, P.B., Grieve, R.A.F., 1977. Shock attenuation at terrestrial impact structures, in Impact and explosion cratering, Roddy, D.J., Pepin, R.O., Merrill, R.B., eds., Pergamon Press, New York, p.687-702.

Schulze, D.J., Helmstaedt, H., 1988. Coesite-sanidine eclogites from kimberlite: Products of mantle fractionation or subduction? Jour. of Geol., v.96, p.435-443.

Shoemaker, E.M., Gault, D.E., Lugn, R.V., 1961. Shatter cones formed by high speed impact in Dolomite. U.S.G.S. Prof. Pap., 424-D, p.365-368.

Smith, D.C., 1988. A review of the peculiar mineralogy of the "Norwegian coesite-eclogite province", with crystal-chemical, petrological, geochemical and geodynamical notes and an extensive bibliography, in Eclogites and eclogite-facies rocks, Smith, D.C., ed., Elsevier, Amsterdam, p.1-206.

Smyth, J.R., Hatton, C.J., 1977. A coesite-sanidine grospydite

from the Roberts Victor kimberlite. Earth Planet. Sci. Letters, v.34, p.284-290.

Speers, E.C., 1957. The age relations and origin of common Sudbury Breccia. Jour. of Geol., v.65, 5, p.497-514.

Stockwell, C.H., McGlynn, J.C., Emslie, R.F., Sanford, B.V., Norris, A.V., Fahrig, W.F., Currie, K., 1970. Geology of the Canadian shield, in Geology of economic minerals of Canada, Douglas, R.J.W., ed., Geological Survey of Canada, Economic Geology Report, p.44-50.

Stöffler, D., 1966. Zones of impact metamorphism in the crystalline rocks of the Nördlinger Ries crater. Contr. Mineral. Petrol., 12, p.15-24.

Stöffler, D., 1971. Coesite and stishovite in shocked crystalline rocks. Lunar Sci. Inst. Contrib., 53, p.5474-5488.

Stöffler, D., 1972. Deformation and transformation of rock-forming minerals by natural and experimental shock processes part I, Behavior of minerals under shock compression. Fortschr. Miner., 49, p.50-113.

Thomson, J.E., 1961. Maclennan and Scadding Townships. Ontario Department of Mines, Geological Report 2, 34p. Accompanied by Map 2009, and 3 charts.

Tschermak, G., 1872. Die Meteoriten von Shergotty und Gopalpur, Sitzungsber. Akad. Wiss., Wien, Math-Naturwiss., Kl., 65, pt.1, p.122-146.

Van Schmus, W.R., 1965. The geochronology of the Blind River-Bruce Mines area, Ontario, Canada. Jour. of Geol., v.73, 5, p.755-780.

Wasson, J.T., Kallemeyn, G.W., 1988. Compositions of chondrites. Phil. Trans. R. Soc. Lond. A., 235, p.535-544.

Winzer, S.R., 1975. Does impact produce chemical fractionation? Abstract, EOS, 56, p.389-390.

Winzer, S.R., Lum, R.K.L., Schuhmann, S., 1976. Rb, Sr, and strontium isotopic composition, K/Ar age and large ion lithophile trace element abundances in rocks and glasses from the Wanapitei Lake impact structure. Geochim. Cosmochim. Acta., v.40, 1, p.51-57.

Wolf, R., Woodrow, A.B., Grieve, R.A.F., 1980. Meteoritic

material at four Canadian impact craters. Geochim. Cosmochim. Acta., v.44, p.1015-1022.

Wright, T.L., Doherty, P.C., 1970. A linear programming and least squares computer method for solving petrologic mixing problems. Bull. Geol. Soc. Amer., v.81, p.1995-2008.

Young, G.M., 1969. Geochemistry of early Proterozoic tillites and argillites of the Gowganda Formation, Ontario. Geochim. Cosmochim. Acta., v.33, p.463-492.